Review

Additive Manufacturing Approaches to Design Pore Structures for Development of Bioactive Scaffolds for Orthopedic Applications: A Critical Review

Mikhail V Kiselevskiy , Natalia Yu Anisimova * , Alexei V Kapustin , Alexander A Ryzhkin , Daria N Kuznetsova , Veronika V Polyakova , Nariman A Enikeev

Posted Date: 30 August 2023

doi: 10.20944/preprints202308.1983.v1

Keywords: additive manufacturing; bioactive scaffolds; porous materials; finite element simulation; pore design; microstructure, biocompatibility; mechanical properties, titanium alloys

Review

Additive Manufacturing Approaches to Design Pore Structures for Development of Bioactive Scaffolds for Orthopedic Applications: A Critical Review

Mikhail V. Kiselevskiy [1], Natalia Yu. Anisimova [1,*], Alexei V. Kapustin [2], Alexander A. Ryzhkin [2], Daria N. Kuznetsova [2], Veronika V. Polyakova [2] and Nariman A. Enikeev [2,3]

[1] N.N. Blokhin National Medical Research Center of Oncology (N.N. Blokhin NMRCO) of the Ministry of Health of the Russian Federation, 115478 Moscow, Russia; n_anisimova@list.ru (N.Yu.A.), kisele@inbox.ru (M.V.K)

[2] Laboratory for Metals and Alloys under Extreme Impacts, Ufa University of Science and Technology, 450076 Ufa, Russia; kapustin129@yandex.ru (A.V.K.), littlepikelet@gmail.com (D.N.K.), vnurik@gmail.com (V.V.P.), nariman.enikeev@gmail.com (N.A.E.)

[3] Laboratory for Dynamics and Extreme Characteristics of Promising Nanostructured Materials, Saint Petersburg State University, 199034 St. Petersburg, Russia

* Correspondence: n_anisimova@list.ru

Abstract: We overview recent findings achieved in the field of model-driven development of additively manufactured porous materials for development of a new generation of bioactive implants for orthopedic applications. Porous structures produced of biocompatible titanium alloys by selective laser melting can present a promising material to design scaffolds with regulated mechanical properties and with capacity to be loaded with pharmaceutical products. Adjusting pore geometry, one could control elastic modulus and strength/fatigue properties of the engineered structures to be compatible with bone tissues, thus preventing the stress shield effect when replacing a diseased bone fragment. Adsorption of medicals by internal spaces would make it possible to emit the antibiotic and anti-tumor agents into surrounding tissues. We critically analyze the recent advances in the field featuring model design approaches, virtual testing of the designed structures, capabilities of additive printing of porous structures, biomedical issues of the engineered scaffolds and so on. A special attention is paid to highlight the current troubles in the field and the ways of their solutions.

Keywords: additive manufacturing; bioactive scaffolds; porous materials; finite element simulation; pore design; microstructure; biocompatibility; mechanical properties; titanium alloys

1. Introduction

With recent progress in additive manufacturing (AM) technology, the number of publications on developing porous materials for biomedical applications exhibits an avalanche-alike growth, as denoted in series of the most recent extensive reviews [1–5]. Advantages of AM approaches to engineer fine-structured, property-controlled and custom-designed products of numerous metallic, ceramic, carbon and plastic materials stipulated development of porous materials capable of replacing affected areas of bones as well as of locally delivering pharmaceuticals. Successful exploring this area demands realization of multidisciplinary approaches joining efforts of prominent researchers in the field of AM technology, computer-assisted design, multiscale simulation, tissue engineering, microstructural assessment, property characterization, biomedical studies, oncologic orthopedy and so on. The present review focuses on the analysis of the newest findings provided by synergetic efforts of different researchers to engineer porous materials by AM and highlights critical issues to be solved on the way to manufacture the advanced personalized bioactive implants/scaffolds for innovative applications in oncologic orthopedy. We overview the benefits of and troubles with (i) AM approaches to print the designed porous structures; (ii) finite-element

 doi:10.20944/preprints202308.1983.v1

simulations of their elastic, strength and fatigue properties; (iii) application of neural networks for thoughtful optimization of the pore geometry for the best performance; (iv) experimental characterization and post-printed treatment of the AM materials, (v) biomedical and clinical issues of AM titanium alloys to fit the requirements of the developed materials to provide necessary osteoconductivity and osteoinductivity required to use the scaffolds as platforms for the local delivery of medical products into an implanted area.

2. Materials for orthopedic implants

Orthopedic implants represent medical devices that facilitate healing bone fractures and defects. Recent developments in AM technology for printing by metals have led to the use of porous structures, which can promote bone ingrowth and biological fixation of medical implants. Bone fractures are the most common injuries in humans. The healing of bone fractures involves a regenerative process that, in most cases, results in the restoration of the damaged bone. However, 5-10% of fractures lead to delayed healing or retarded bone union, especially in cases of comorbidities such as diabetes [6,7]. Complex or compromised bone fractures (i.e. fractures larger than a critical size of <4 cm, with severely damaged surrounding tissues), comorbidities, and improper initial treatment increase the risk of delayed healing and non-union [8]. Additional indications requiring bone healing include bone defects resulting from bone tumor resections, infections, or in the context of prosthetics. Damaged joints and degenerative diseases may require arthrodesis, the artificial induction of a joint bridge between two bones, also known as fusion. Arthrodesis is most commonly performed on spinal joints, the wrist, ankle, and foot. All these conditions require the filling of bone defects and bone grafts. Global sales of orthopedic products are estimated at $55.5 billion in 2022 and include all products used for the treatment of fractures, both internal and external: plates, screws, intramedullary nails, pins, wires, staples, and external fixators; spinal implants and instruments [9]. Patients with various bone diseases, particularly with injuries, require bone defect replacement. Among all musculoskeletal injuries, fractures of long bones account for 17-49% of cases, and the majority of these patients require osteosynthesis using intramedullary implants and/or fixation devices [10,11].

The need for bioactive implants is due to the prevalence of bone sarcoma, characterized with high morbidity and mortality, especially for children and adolescents [12]. The most common types are osteosarcoma (56%), chondrosarcoma (10%), and Ewing's sarcoma (34-36%) [13]. Here, Ti and Ti-based alloys have been considered not only as materials for orthopedics but also as drugs delivery systems for local chemotherapy/immunotherapy. Despite the advancements in modern oncology, systemic chemotherapy remains the most commonly used method for treating malignant tumors. However, when administered intravenously, only a small portion of the anti-tumor cytostatic agents reach the tumor, affecting normal tissues and leading to undesirable side effects. Local chemotherapy utilizing drug delivery systems is a highly promising method for enhancing the effectiveness of anti-tumor treatment and minimizing systemic side effects [14].

Thus, in various diseases and pathological conditions of the bone tissue, there is a need for replacement of bone defects. Approaches to creating biocompatible materials will be promising not only as bone prostheses and fixation elements, but also for the development of drug delivery systems to the area of tumor processes. This approach will significantly increase the demand for such structures for the purposes of oncology, traumatology, and regenerative medicine.

Biocompatible metals and alloys (such as Ti, Ta, Co-Cr, etc) represent the most popular materials used to manufacture permanent orthopedic devices. Among them, Ti and Ti-based alloys, which undergo morphological and/or chemical surface modifications, are most often used materials for dental and orthopedic implants [15]. However, these materials have higher elastic moduli (100-140 GPa for Ti alloys [16], 210-253 GPa for Co alloys [17], and 190-210 GPa for stainless steel [18]) than that of bone (0.5-20 GPa) [19]. Such an incompatible elastic modulus with bone can lead to the manifestation of the stress shielding effect [20], and as a result, to implant loosening or autogenous bone fracture. Due to the poor biomechanical compatibility of traditional metal implants, the interfacial adhesion between bone tissue and the implant is unstable. Most full-density metallic

 doi:10.20944/preprints202308.1983.v1

implant materials used in clinical practice still suffer from problems such as implant infection, unstable interface with host tissue, biomechanical mismatch in elastic modulus and limited service life. Due to these clinical shortcomings, current research is focused on developing novel devices that can prevent postoperative infection, provide early stability and rapid healing, and enable remodeling of surrounding tissue structures [21].

As a result, in recent years, there has been great interest in engineering metallic materials with a porous structure, which allows for purposeful tuning of their mechanical and functional performance. By varying the size and fraction of pores, it is possible to design a metallic implant with optimal mechanical properties and compatibility with bone tissue, which can prevent osteonecrosis and disruption of osteointegration [22]. In addition, the internal porous structure promotes adhesion, proliferation, and differentiation of mesenchymal stem cells in the osteogenic direction. The porous structure also provides a larger surface area for vascularization and osteointegration, promoting biological fixation of the implant and bone [23].

AM technologies open cardinally new prospects to design porous structures for advanced personalized biomimetic orthopedic implants of the next generation [1–5]. AM allows printing multifunctional implants with thoughtfully designed complicated internal geometry which cannot be manufactured through traditional approaches. AM approaches are capable of tailoring materials to be most compatible with the replaced bone fragments by mechanical, chemical and biological properties. AM is also very flexible in printing by various materials. Biomedical Ti-based alloys, Ta, Co-Cr alloys have been considered as an attractive base for AM-driven orthopedic solutions thanks to the unique combination of functional properties including excellent biocompatibility [24], high fracture toughness [25], good wear and corrosion resistance [26], adjustable stiffness to prevent stress shielding effect [27]. Recent advances in optimization of AT processes to design a topology of porous structures allowed to find promising paths to fit multiple demands for desired combinations of mechanical and biological parameters of porous implants ensuring successful bone regeneration and tissue integration [28,29] as well as reducing stress shielding effect [30]. Tunable pore architecture enables also enhancing permeability and, hence, better osteointegration [31,32].

However, there are still many troublesome issues on the way to produce reliable medical products of porous structures. 3D printing is known to introduce both internal defects and geometrical deviations in the manufactured workpieces, caused by quality of powders, non-optimal processing parameters and native peculiarities of AM technology [33]. These features may affect the functional performance of the printed articles and in order to achieve high-quality products laborious monitoring procedures are required involving instrumental control and computer-assisted engineering including machine learning [34,35].

Thus, to solve the problems above, it is necessary to implement the correct choice of materials, optimize the design, and employ advanced manufacturing technologies, which require a deep interdisciplinary understanding of the structure-topology-property relationships from both physical and biomedical points of view. Due to these reasons, there is still limited success in using AM for the development of specific biomedical products. Therefore, the comprehensive task of developing bioactive implants using AM technologies is one of the most relevant challenges in the fields of life sciences and materials science. Below we consider specific issues related to AM production of bioactive scaffolds for orthopedic oncology from the viewpoints of materials science and biomedicine.

3. Features of AM techniques as related to printing porous structures

Modern AM technologies offer a number of approaches to produce wide range of materials with pre-defined internal geometries, dimensions and AM-induced microstructures. This subsection focuses on the AM solutions for manufacturing porous titanium alloys approved to be used in articles for medical applications.

 doi:10.20944/preprints202308.1983.v1

3.1. AM techniques to print porous biocompatibe products of Ti alloys

Currently, the printing of porous materials is one of the most important tasks in the field of additive manufacturing. In general, porous structures have a wide range of applications, including biomedicine, energy, electronics, and many other industries [36]. Creating such structures for medical applications requires specialized AM approaches allowing to print three-dimensional objects with high precision [37–39].

AM can provide printing complex three-dimensional structures by progressive layering and melting powders with a programmed beam trajectory [36]. There are numerous types of AM printing, each with its own ups and downs depending on the specific application [40]. For printing fine structures with a complicated geometry, AM methods based on the fusion of ultra-dispersed powders are typically used.

Laser-based technology, specifically, selective laser melting (SLM) also often denoted as as laser power bed fusion , and electron beam melting (EBM) techniques, are preferred for applications in biomedicine as they enable the printing porous structures with the finest available dimensions of pores (starting from 20-25 μm) [41] of high-quality biocompatible alloys. These techniques enable producing precise and smooth surfaces but require high precision positioning and high accuracy laser control [40,42–44].

Printing parameters for porous structures can significantly vary depending on the material and application [45–48]. Each AM technique has particular features to be considered when manufacturing any specific target product, such as porous articles of Ti alloys. The AM powders must be produced of high purity biocompatible materials officially approved for medical purposes according to the national standards. 3D printer should be equipped with a laser characterized by high power and printing accuracy due to the high melting temperature of Ti alloys. Powders with the least possible particle size are required for printing percolating porous structures with sophisticated internal geometries [48]. Limitations on the laser beam size and accuracy of the focusing system are imposed by the dimensions of the working area. The system must provide beam focusing over surfaces longer than 150 mm without power loss [49]. The powder particle size and the thickness of the deposited layer must provide the prescribed printing accuracy defined by cell wall thickness, and the pore dimensions [50] – the beam size and a focusing accuracy have to match the powder size.

To be specific, despite the high accuracy of the modern SLM/EBM 3D printing systems, the quality of printing depends on a number of factors:

1. Powders for SLM printing of titanium medical devices must meet strict requirements (purity, density, homogeneity, particle shape and size) [51,52] to ensure high print quality, biocompatibility, and product reliability [53,54]:
    - Homogeneity: Powders must be homogeneous in terms of particle shape and size. This is necessary to ensure uniform sintering and to obtain smooth printed surface.
    - Purity: Powders must not contain any impurities inherited from atomizing processes which can affect the biomedical and mechanical response of the products. This avoids the risk of rejection, increases service life, and accelerates osseointegration.
    - Density: The density of powders should be enough to ensure proper sintering and to avoid the formation of voids and other printing defects.
    - Particle size: The powder particle size should be small enough to ensure good adhesion to the platform and prevent the formation of internal defects in the products. Particle size also defines the minimum possible inaccuracy of the printed structures as compared with the designed ones.
    - Particle shape: The particle shape should be spherical or close to spherical to ensure uniform sintering and form smooth printed surfaces.
2. AM equipment settings. Laser processing parameters, such as power and speed, should be properly adjusted to ensure optimal powder melting and solidification. Before the final production, the printer settings should be calibrated for each particular material and design. Testing different parameters and settings can help determine the optimal settings for a specific task and material [55].

 doi:10.20944/preprints202308.1983.v1

3. Environmental conditions, such as humidity, dustiness, and temperature in the facility, can have an impact on the print quality. It is important to ensure that proper environmental conditions are monitored during SLM printing [56].

3.2. Features of as-printed materials

Functional properties of titanium alloy products produced by SLM methods, as well as the their density, depend not only on the quality of the starting powder, but also on the technological parameters of the selective melting process [57–59] For example, varying the laser power, scanning speed and thickness of the fused layer have a significant effect on the homogeneity of the structure and properties of printed samples as well as formation of voids, cracks and unmelted particles. High residual stresses may arise due to heterogeneous heating and rapid solidification during SLM process, while post-printing annealing can also reduce the strength of the printed articles [60]. Another issue that may affect the scattering of samples' properties is the location of the product on the printing platform. In particular, the relative elongation of differently positioned test specimens with the same printing parameters varied from 5 to 17 % depending on their location [58].

When scanning at low speeds, melt bath instability can be observed due to hydrodynamics, which leads to inhomogeneous structure formation. However, with increasing scanning speed combined with high laser power, thermocapillary effects may occur, which may also lead to instability [61]. Low laser power results in the formation of high porosity of products due to incomplete melting of the powder layer and poor adhesion of the cladding layer to earlier layers [62]. Increasing the power can again solve this problem, however, local injection by a high-energy laser beam leads to heterogeneous heating of the metal, resulting in a thermal gradient, and as a consequence, anisotropy of the structure and high residual stresses [62,63].

The microstructure of the AM materials is usually characterized by a fine-grained structure that arises from the rapid solidification of melted metal powders. The size and morphology of the grains and fragments can vary depending on the material composition, laser parameters, and heat transfer during the process [59]. Phase composition can also be affected by the printing processes. At high cooling rates, depending on the class of a Ti alloy, a structure from quasi-equilibrium Widmanstett structure consisting of α-phase plate packets [64] to non-equilibrium fine-dispersed acicular martensite structure [65] with a high density of dislocations and twins [66] can be formed out of β-phase grains. The formation of such non-equilibrium structures leads to a significant increase in the strength and a loss in ductility of printed Ti alloys compared to those produced by traditional methods of metal forming [67,68]. In order to compensate the effect of AM-induced microstructural features, specified heat treatments in the form of tempering or ageing are applied [69,70].

The aforementioned factors can influence the mechanical properties of the AM-produced materials. In addition, SLM-printed specimens can exhibit a specific crystallographic texture with preferential alignment of grains along the construction direction which introduces considerable anisotropy of mechanical properties, especially in materials with a low symmetry such as Ti alloys [71].

The SLM 3D printing process can result in heterogeneous surface roughness due to the layered deposition of material which is important from biomedical point of view. To improve surface quality, post-processing methods such as mechanical finishing, chemical or electrolytic polishing, or abrasive blasting can be used. The texture and topography of the surface can affect the wettability, adhesion, and corrosion resistance of printed materials [72].

Additional trouble with the printed porous structures is related to the intrinsic feature AM technology: unmelted particles can be trapped in the internal cavities of the printed product [73]. The presence of trapped powders is undesired for the articles designed for medical applications and cleaning by powder recovery systems is required. Standard techniques such as air jet cleaning might be insufficient to release trapped powder from porous specimens with complicated internal geometry[73] and chemical or ultrasound vibration must be applied. In their turn, these additional treatments might change the primarily designed cellular geometry.

 doi:10.20944/preprints202308.1983.v1

The issues above can significantly impact the mechanical properties and functional characteristics of printed components. Therefore, it is crucial to optimize process parameters, including laser power, scanning speed, and powder feed rate, to minimize the number of defects and ensure material integrity [74]. Specific features of the AM alloys such as refined microstructure, increased defect density, changed phase composition and AM-induced texture are very important to be taken into consideration in computer-aided design of the porous structures.

4. Computer-assisted design of pore/cell geometry

Development of AM technologies impossible without implementation of modern modeling approaches which require equipment with high computational performance. Bioactive scaffolds need in a purposeful design of porous structures with fine sophisticated geometry to satisfy numerous requirements of regulated mechanical properties, osteo- inductivity and conductivity, biocompatibility and permeability.

4.1. Design of cell geometry to build up porous products

Understanding on how the design of porous structures defines the properties of printed articles is highly important to achieve high quality medical products with desired performance. The models of porous structures are characterized by the spatial arrangement of cells consisted of pores and inter-pore walls, the pore size and their distribution, cell geometry, configuration of inter-pore partitions, the type of pore relief, etc. [75]. The mechanical and physical properties of porous structures explicitly depend on the topology of the cells. The analysis of the relationship between structure and properties shows that the mechanical and physical properties of porous materials depend not only on the chemical composition of the material but also on the geometric characteristics of the elementary cell or cell blocks forming the porous/cellular material.

At the same time, it should be noted that for the normal development of bone tissue, porous materials must provide for the diffusion of fluids and nutrients, as well as the removal of metabolic waste [76–78]. It should also be considered that the structure of the material is important for the functioning of bone tissue during and after the process of regeneration and remodeling [79–81]. Therefore, the following parameters should be taken into account during the optimization of the structure of porous materials: porosity, permeability, and mechanical properties (stiffness, viscosity, and elastic modulus) [82].

There are various methods for designing porous materials, from optimization approaches to top-down or bottom-up approaches [83]. Among them, the most popular approach for designing porous structures is the mathematical representation of cellular structured materials based on triply periodic minimal surfaces (TPMS).

This approach has shown a high degree of cell migration while providing a high degree of mechanical and structural stiffness for porous materials [84]. This approach is chosen for its topological features and the associated geometric characteristics, such as a high surface-to-volume ratio and interpenetrating networks of pores and voids.

The high surface-to-volume ratio and the presence of interpenetrating networks of pores and voids allow for the maximum utilization of base materials, such as titanium and its alloys, in the creation of porous materials. This architecture also enables the storage of large volumes of liquids, such as medications and columnar cells, in a small volume of porous material. This design approach provides lightness while maintaining the necessary stiffness, and is suitable for additive manufacturing [82,85,86].

TPMS is an infinite and periodic curved surface that does not contain self-intersecting fragments and allows for the creation of homogeneous structures. These surfaces have crystallographic group symmetries: cubic, tetragonal, hexagonal, rhombic. TPMS is formed using an implicit method, i.e. using unambiguous functions of three variables, and the surface is defined by three axis-parameters [87] (x, y, z). An example of describing a TPMS surface is an equation of the type (1):

$$\cos \alpha x + \cos \beta y + \cos \gamma z = c, \quad (1)$$

Preprints (www.preprints.org) | NOT PEER-REVIEWED | Posted: 30 August 2023 doi:10.20944/preprints202308.1983.v1

where α, β, γ are parameters that determine the sizes of the base cell along the x, y, z axes, and the constant c determines the density of the structure. That is, this equation represents a set of trigonometric functions that together satisfy the equality $\phi(x, y, z) = c$, and this function $\phi(x,y,z)$ is an isosurface evaluated by the isovalue c.

In the case of "c = 0", the obtained isosurface divides the space into subregions of equal volume. The volume of these subregions varies with the constant "c", such that these volumes can be expanded or compressed by displacing from zero value in the normal or opposite direction.

Creating a lattice TPMS structure in the case of "c = 0", i.e. based on zero thickness, is possible using 2 approaches [88,89].

1) Skeleton structure (Solid-Networks, $\varphi < k$ or $\varphi > k$). In this case, one of the volumes bounded by the minimal surface is considered as a solid region, while the other is considered as an empty region. This is achieved by considering the volume bounded by the minimal surface such that $\varphi(x, y, z) > k$ or $\varphi(x, y, z) < k$, in order to create the lattice TPMS structure.
2) Sheet structure (Sheet-Networks, $k \leq \varphi \geq k$). In this case, the creation of the lattice structure of TPMS is achieved by creating a double surface and transforming it into a solid structure based on the blending of isosurfaces along its normal and anti-normal direction by solving $-k \leq \varphi(x, y, z) \leq k$. The resulting structure is a lattice created based on the isosurface by thickening it within a certain limit $-k \leq \varphi(x, y, z) \leq k$.

Sometimes, the description of the parametric equation of a TPMS structure indicates a grading of relative density "s" [89,90]. This characteristic can be understood as the density of the resulting lattice divided by the density of the base structure from which the lattice is generated. It also represents the fraction that represents the volume of the solid lattice relative to the volume of the cell space occupied by the lattice.

However, due to the characteristics of the parametric description of TPMS surfaces, there is a strict interdependence between the size of the pores and the walls of the cells, which are based on an implicit function (cos(x, y, z) or sin(x, y, z)) and expressed as a set of constants (α, β, γ, c, k, s). Thus, variable density, cell size gradients, hybridization, hierarchy, etc. are achieved by controlling the implicit function (cos(x, y, z) or sin(x, y, z)) and the constants (α, β, γ, c, k, s) in the set of levels.

Currently, the most widely used programs for creating porous structures include Triangulatica, nTopology, Gen3D Sulis, Autodesk Fusion 360, Netfabb, etc. as well as the MSLattice plugin which was used to create models in MATLAB, SpaceClaim, and "OpenSCAD" – see the examples in Figure 1. The following parameters are set for the sample diameter - 6mm, height - 9mm.Different parameters for the 11 created models are provided in the following tables (Table 1). The Diamond, IWP, and Gyroid models use the approach of creating a lattice structure TPMS - Sheet-Networks ($k \leq \varphi \geq k$).

Table 1. Model parameters.

Model	Expression
Diamond	cos X cos Y cos Z – sin X sin Y sin Z =c
IWP	2 (cos X cos Y +cos Y cos Z + cos Z cos X) − (cos 2X +cos 2Y +cos 2Z) = 0
Gyroid	sin Y cos X + sin Z cos Y + sin X cos Z = 0

Preprints (www.preprints.org) | NOT PEER-REVIEWED | Posted: 30 August 2023 doi:10.20944/preprints202308.1983.v1

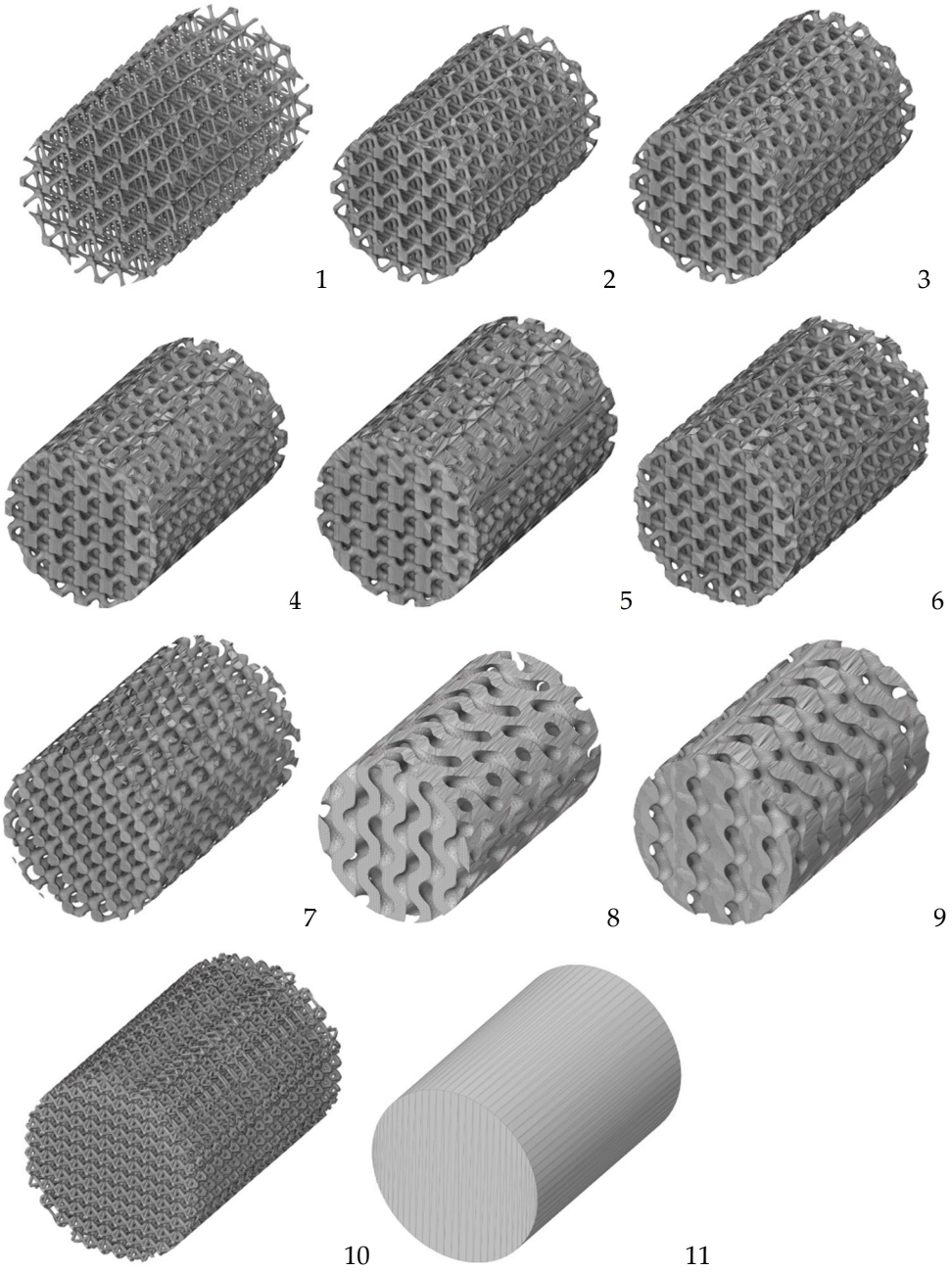

Figure 1. Models of a cylindrical sample built using TMPS models with different parameters featuring the effect of (1-5) the different pore/wall ratio; (6-9) different cell designs; (11) fully dense model.

4.2. Consistency of the designed and printed structures

When printing objects, there can be a number of issues related to both the design of porous materials and the characteristics of 3D printing. The most widely used format in AM solutions is STL (stereolithography), which is universal for most 3D printers and is part of a developed ecosystem that includes software infrastructure and solutions for model development. However, STL has limitations in terms of the amount of saved information, as it only includes a description of the external surface and shape of the 3D model and does not contain, for example, data on the color or material of the samples. Additionally, models are usually saved in the STL format from various applications, making it difficult to edit the final result, while inaccuracies in the original design can cause gaps and overlaps on connecting surfaces. Additionally, high-precision models of complex systems such as porous materials usually occupy large volumes (over hundreds of megabytes) and their exploring requires high-performance computers [91].

Another problem is the mismatch between the designed and printed models, which is related to the implementation of the 3D printing process: uneven solidification of sintered powders; the presence of residual stresses, which can cause noticeable deviation of the product's geometry from the desired shape; inaccuracies associated with the finite size of the laser beam, comparable to the size of the printed pores (20-50 microns) [1]. To achieve in practice a product geometry that accurately corresponds to the one designed in simulation, preliminary research is necessary for targeted design of porous structures. Assuming that the studies on developing pore geometry for superior functional performance of bioactive scaffolds require considering numerous sets of parameters, application of neural networks-based solutions seem to be promising for further progress in the area [92]. The related recent works are briefly reviewed below.

4.3. Neural networks to optimize porous structures for biomedical applications

Nowadays artificial intelligence (AI) plays an increasingly important role in various fields, and healthcare is no exception. The first place where AI can play an important role be materials science and physical approaches to the microstructure of materials [93,94]. Through computer modeling, data analysis and machine learning, artificial intelligence can optimize the parameters of materials, which in theory should lead to improved biomechanical properties and biocompatibility (which is what we are striving for). AI can simulate many different options in a short amount of time and predict which of those options will work best, resulting in lower research budgets.

The second area where AI will help a lot is the engineering approach to product design [95]. Using 3D computer models and additive technologies, artificial intelligence can create more complex and accurate implant designs than humans, tailored to the individual needs of the patient. This principle will allow us to look for individual solutions that will most accurately suit the patient and his specific situation.

The third area in which AI has great potential is biotechnological and medical approaches to the impregnation (pore filling) of implants with bioactive substances. Ideally, a separately created neural network can help choose the best medicine for successful treatment. In addition, AI could predict the effectiveness of various drugs, reducing the time for clinical trials and accelerating the introduction of new treatments [96].

Let us consider in detail how exactly the use of artificial intelligence can contribute to our project. To begin with, it is worth noting that neural networks can assist in predicting print quality [97]. Machine learning methods can distinguish which print configurations will theoretically lead to the highest quality result. However, although the neural network can predict this, it provides recommendations based on the available data and is not able to infer the necessary ideal parameters on its own. The result obtained with the help of neural networks does not claim to be absolute accuracy. In addition, neural networks contribute to the analysis of scaffold parameters and the determination of their influence on the processes of angiogenesis and interaction with tissues [98]. This allows a deeper understanding of the mechanisms of interaction between materials and biological systems and adapts the design of scaffolds to optimal requirements.

Note that the absence of an expert physical model can lead to limitations in the analysis of the physical properties of materials [98]. Also, limited data may reduce the generalization threshold of the results in the projection to any other conditions.

It should be borne in mind that the use of neural networks does not exclude the importance of using expert models. Some parameters, such as reactivity and biocompatibility, can have a significant impact on the development of bioactive porous scaffolds and cannot always be fully considered by neural networks. In addition, it is important to remember that with a limited set of machine learning models, this does not contribute to a wider consideration of certain more complex architectures of neural networks [94].

Neural networks are also capable of processing large amounts of data, making it possible to collect and analyze information about the results of clinical trials and the effectiveness of new implants. This can speed up obtaining regulatory approval by providing evidence of the effectiveness of developed products.

 doi:10.20944/preprints202308.1983.v1

In addition, the use of AI also contributes to accessibility. Automating multiple processes and reducing implant development and manufacturing times will result in cost savings, making the final product accessible to more patients.

Thus, artificial intelligence can play an important role in the successful implementation of projects aimed at developing advanced bioactive implants for healthcare. The application of AI in various aspects will lead to process optimization, increase in efficiency, and facilitate the integration of solutions into clinical settings. The result will be a better quality of life for patients and more effective treatment.

Creating a full-fledged artificial intelligence to create bioactive implants with a porous structure requires complex approaches, including the use of genetic algorithms, machine learning, and deep neural networks. It also requires integration with medical data to create patient-specific solutions.

Let us highlight some other pros and cons of using artificial intelligence in the production of bioactive scaffolds and other related areas of research.

Key benefits of using artificial intelligence (AI) in medicine:

- Improved diagnostic function. AI analyzes medical data, images and symptoms with high accuracy and is useful for early detection of diseases and more accurate diagnosis.
- Optimized treatment. AI can create a personalized treatment plan for each patient based on their unique characteristics and response to medications.
- Fewer mistakes. AI can help minimize diagnostic and treatment errors, as well as improve the quality of care and patient safety.
- Speed up research. AI can process and analyze vast amounts of data, accelerating the research and development of new treatments.
- Automation of tasks. AI allows the automation of routine tasks such as processing medical records, freeing healthcare workers to focus on more complex tasks.
- The main disadvantages of using artificial intelligence in medicine:
- Lack of transparency. Some AI algorithms are difficult to understand and explain, which creates trust issues between medical professionals and patients.
- Ethical issues. The use of AI in medicine raises important ethical issues such as data privacy, decision making, and liability for errors.
- Data dependencies. The performance of AI in healthcare depends on the quality and quantity of data available. Inaccurate or limited data may affect the accuracy of your results.
- High cost. Developing, deploying, and maintaining AI systems in healthcare can be costly, especially in smaller clinics or countries with limited resources.
- Responsibility for errors. The use of AI in medicine raises questions about who is responsible for errors made by automated systems, which can be legally difficult.

It should be noted that the development of a full-fledged artificial intelligence for the creation of bioactive implants with a porous structure requires a deep and complex analysis of data and algorithms. Creating such a solution requires a multidisciplinary team of biotechnologists, engineers, programmers, and medical professionals. It is also important to consider ethical aspects and safety when using neural network-generated models.

The development of innovative solutions in the fields of healthcare and medical technology is one of the major trends in modern academic research. Personalized medicine, improving quality of life and innovative therapies have become paramount, requiring the integration of multiple disciplines to achieve optimal results.

In this context, special attention has been paid to the development of biomedical implants for targeted drug delivery and treatment of bone defects, including bone defects associated with oncological diseases of the musculoskeletal system. Such implants, with their ability to control drug release, are innovative tools for effective and personalized therapy.

Let us review existing approaches to model the release of drugs from pores in bioactive implants and describes the methodology and stages of their creation using the latest engineering and biotechnology methods. Based on the multi-sphere approach, the physical, chemical, and biological properties of materials and their interaction mechanisms with drugs should be considered. This

Preprints (www.preprints.org) | NOT PEER-REVIEWED | Posted: 30 August 2023 doi:10.20944/preprints202308.1983.v1

research is a step forward towards more effective and personalized treatment of musculoskeletal disorders and opens new frontiers in biomedical science and engineering.

Numerous studies in the field of biomedical technologies demonstrate the complexity of the path to the development of the most appropriate solutions in the context of the topic under study. The ability to simulate natural biological structures (in our case, bone structures) when creating implants and optimizing them is an important prospect for regulating biological processes in the body [99]. This appears to be a complex task requiring consideration of various aspects. For such studies, the method of photocuring 3D printing may be suitable. Photocuring 3D printing technique is a method of creating three-dimensional objects using light, which uses a type of liquid resin that becomes solid when exposed to light [100]. This resin is placed on a platform, light is directed onto it so that it falls only on the right places. When light hits the resin, it begins to harden and become part of a solid body. After that, the platform is lowered, and the process is repeated until the entire object becomes monolithic. However, this method can hardly be applied for the case of metallic materials.

In the context under study, innovations in fabrication methods are quite capable of opening new horizons for the creation of more complex and precise structures. But despite the existing prospects, the lack of a complete understanding of the mechanisms of interaction between implants and cells limits the use of the above technologies [101].

With the development of methods for characterizing the porosity of materials (a digital imaging method for characterizing the porosity and pore structure of materials based on the use of image processing algorithms adapted for specific sequences), it becomes possible to determine the structural features of porous implants more accurately. New approaches to analysis and software solutions provide the possibility of a more detailed and faster analysis of the structure of materials. This creates the basis for further expansion of the scope of various methods, including soft materials and materials in which the structure plays a key role [101].

The creation of new types of porous structures is an additional step in obtaining successful biomedical engineering solutions. A general approach to construct neural networks for cell geometry optimization is shown in Figure 2 [92]. However, the use of these structures is at a crossroads in identifying both advantages and, of course, limitations. This is an important area of research that requires additional in-depth analysis and verification of effectiveness in real conditions [102].

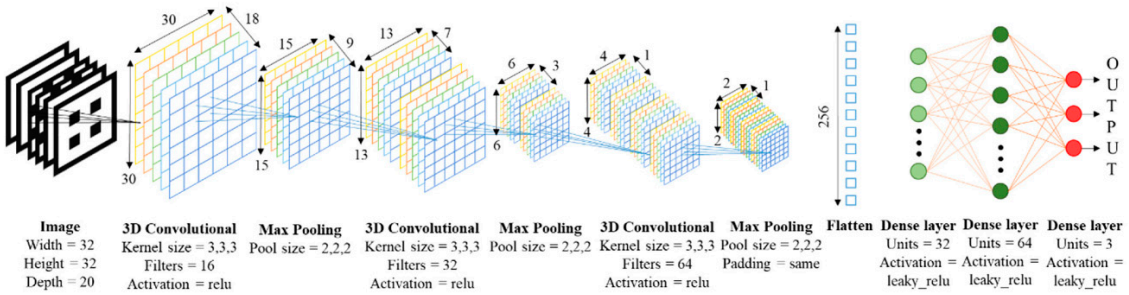

Figure 2. A general scheme including block diagram, structure and details for the 3D convolutional neural network: from 3Dslices models to useful performance properties of porous structures. The figure is reproduced from [92].

As a case study, modeling the release of drugs from porous bioactive implants requires consideration of various input data and factors that influence the release kinetics. Consider what data and factors need to be considered when modeling this process.

Input data.

- Drug inclusion mode [103].
- Shape of the implant. Shape, size, and configuration of porous implants. This includes parameters such as pore diameter and depth, pore location, total pore volume, and total implant surface [104].
- Material microstructure. Porous implants may have different microstructures and phase compositions, which may affect their ability to interact with or release drugs.

 doi:10.20944/preprints202308.1983.v1

- Physical and mechanical properties of materials. It includes parameters such as material density, strength, elasticity, and hardness. These properties can affect the material's ability to retain and release drugs over time [105].
- Chemical properties of materials. A material's chemical composition can affect drug interactions and stability.
- Physicochemical properties of medicinal products. Parameters such as water solubility, particle size and diffusion rate. These properties determine how the drug penetrates the pores of the implant and how quickly it is released.

Factors affecting the emission rate.

- Pore size and shape. Large, open pores can provide faster drug release rates than small, closed pores.
- Porosity of the material. Greater porosity increases the availability of interactions with the drug on the material surface, thus increasing the release rate.
- Drug concentration. A high drug concentration within the pores of the implant can accelerate the release process.
- Physicochemical interactions: Interactions between drugs and implant materials can affect drug release.
- Drug diffusion. The rate of drug diffusion through the implant material determines how quickly the drug is released.
- Environmental conditions. Temperature, humidity, and other environmental conditions can affect drug diffusion and release from implants.

Studies on key aspects of drug release from porous implants have confirmed the great potential of porous implants as innovative tools for personalized medicine and improved treatment outcomes. Combining additive technology and biotechnological methods with computer simulation makes it possible to create biomaterials with optimal properties for the controlled and prolonged release of drugs.

The physical and chemical properties of porous materials (porosity, pore size and shape, surface properties, implant density and thickness, etc.) have a significant impact on drug diffusion mechanisms and their release kinetics. It is important to consider material-drug interactions as well as environmental factors such as temperature and viscosity.

The use of porous implants for targeted drug delivery is a promising approach in modern medicine. It overcomes many of the limitations of conventional therapies and provides long-term drug efficacy at the target tissue. This approach is of particular importance in the treatment of bone malignancies, where precise and long-term delivery of anticancer agents is critical.

Simulation of drug release from porous implants requires a complex interdisciplinary approach. The combination of computer modeling, engineering methods and biotechnology methods allows you to create biomaterials with optimal properties that allow you to control the rate and duration of drug release. This opens new perspectives in the development of personalized and more effective treatments for diseases of the musculoskeletal system. Such innovations can significantly affect medical practice and improve patient outcomes.

5. Biomimetic scaffolds for bone tissue engineering: biomedical issues

Among the modern AM technologies emerging for bone tissue engineering, bioprinting methods allow for the production of biomimetic matrices. Although research is still not at the stage of clinical trials, intensive work in this field continues. Bioprinting is based on the precise deposition of a composite biomaterial, consisting of a combination of hydrogels, cells, and, in some cases, growth factors [106]. This assembly is commonly referred to as “bioincs,” and there are several AM approaches used for bioprinting [107]. To enhance mechanical stability, the structure is usually crosslinked with ultraviolet light, chemicals, or heat [108]. Hydrogels such as collagen, alginate, or hyaluronic acid are the most commonly used materials as bioincs, as they provide an extracellular matrix-like environment for embedded cells and are capable of biodegradation [109]. To stimulate bone tissue regeneration in bioprinting, an additional cellular component is used: mesenchymal stem cells, umbilical cord stem cells, and endothelial stem cell precursors, which are used for

 doi:10.20944/preprints202308.1983.v1

neovascularization purposes [110]. Hydrogels used for bioprinting provide the extracellular environment for cells, but maintaining their viability remains a key challenge in this technique. Another important limitation of bioprinted constructs is the insufficient mechanical strength of hydrogels. Stitching the hydrogel can reduce the viability and functionality of cells, so stronger materials can be added to the hydrogel to improve their properties. For example, Lin et al. [111] created a composite porous bone scaffold consisting of collagen and hydroxyapatite in a 1:2 ratio to replace large bone defects. To stimulate vascularization, Park et al. developed a hydrogel structure containing vascular endothelial growth factor (VEGF) [112]. Bioceramic implants composed of calcium and phosphate have good bioactivity and biodegradability. Bioprinting allows for the reproduction of the architecture of native bone using biocompatible materials and cellular components. However, despite their undeniable advantages, biomimetic degradable matrices have significant drawbacks due to their insufficient mechanical properties, and the gradual biodegradation of the implant can lead to implant failure [113].

5.1. Porous matrices

Additive manufacturing methods are widely used to obtain porous metallic structures, allowing for the production of materials with controlled microarchitecture [114]. One such method is selective laser melting (SLM), which enables the creation of complex metallic products [115,116]. Porous biological metallic matrices built using the SLM method have shown promising results in both in vitro and in vivo studies [117]. Porous metal scaffolds are already being used in orthopedics for the implantation of artificial joints and for the reconstruction of bone defects caused by infection, trauma, or tumor resection [118]. The porous structure can reduce risks associated with the stress shielding effect by matching the mechanical properties of the bone and promoting osteointegration in the bone-implant contact zone, providing the transport of nutrients necessary for the viability and differentiation of precursor osteocyte cells. Unlike ceramics and polymers, porous metallic materials have the advantage of balanced mechanical properties and a unique skeletal structure, which expands their application possibilities in orthopedics [119]. Metallic matrices can have a homogeneous or irregular pore size [120,121]. Homogeneous pore size allows for controlled porosity, providing predictable mechanical properties and scaffold biocompatibility [122,123]. However, human trabecular bone does not have a consistent porosity, so homogeneous porous matrices are not optimal for cell adhesion and proliferation. On the contrary, irregular porous structures, similar to the spongy structure of bone, enhance the biocompatibility of porous matrices and are more favorable for cell growth [27,124,125]. Most non-uniform porous matrices were obtained using the reverse engineering method based on CT imaging, which allows for the simulation of the microarchitecture of natural bone [126]. The mathematical modeling method based on Voronoi-Tessellation enables the construction of approximate models of biomimetic heterogeneous porous materials [127,128]. Methods based on Voronoi-Tessellation not only optimize the microarchitecture of the matrices, but also regulate the mechanical properties (elastic modulus and compressive strength) of the porous matrices, which is important for bone tissue engineering [129]. Several research groups have used the Voronoi-Tessellation method to design biomimetic porous matrices. In particular, Fantini et al. [130] created fully connected porous matrices with a trabecular structure and individual geometry. Gómez et al. [131] modeled the trabecular bone structure based on Voronoi-Tessellation using micro-CT, in accordance with the key histomorphometric properties of trabecular bone. However, the authors did not provide data on the mechanical characteristics and biocompatibility of these Ti-based trabecular scaffolds. Wang et al. developed approaches to create porous titanium matrices with irregularity in the porous structure based on Voronoi-Tessellation, reproducing the natural trabecular bone. The method allowed for the production of matrices with a gradient distribution of porosity ranging from 60% to 95% and pore sizes from 200 μm to 1200 μm [129]. In vitro studies of the titanium porous matrices showed that the fabricated SLM irregular Ti-6Al-4V matrices based on Voronoi-Tessellation exhibited good cytocompatibility and could be considered promising for orthopedic applications. It has been found that pore characteristics and surface properties significantly influence cell adhesion,

 doi:10.20944/preprints202308.1983.v1

proliferation, and differentiation on matrices [122], and cell colonization of matrices is associated with local permeability, which depends on specific surface area and porosity [132].

5.2. Cell geometry

Early studies of materials with different pore sizes have shown that the optimal pore radius for bone ingrowth is 50 μm and can reach up to 150 μm [133–135]. According to Lu et al., human osteoblasts can penetrate, colonize, and proliferate inside macro-pores, with a favorable size of over 40 μm [136]. Later, Itala et al. investigated laser-perforated titanium matrices with pore sizes of 50 μm, 75 μm, 100 μm, and 125 μm, and found the formation of osteonal structures even in the smallest openings, leading to the conclusion that pore size within this range does not affect bone ingrowth in perforated titanium matrices [137]. Similar results have been obtained in several other studies, considering the optimal matrix pore size to be within the range of 50 μm-100 μm [138,139]. Xue et al. investigated the influence of pore size of porous titanium on cell penetration and bone ingrowth. The results showed that porous scaffolds with a pore size of 188 μm were covered with cells, but there was a disruption in oxygen and nutrient exchange, leading to cell death within the matrix, and the optimal pore size was found to be over 200 μm [140]. Knychala et al. [141] implanted hydroxyapatite (HA) matrices with the same pore size (500-600 μm), but different strut sizes (100, 120, 150, and 200 μm), and HA matrices with the same interconnection size (120 μm), but different pore sizes (400-500 μm, 500-600 μm, and 600-700 μm), into distal defects of rabbit femoral condyles. The authors obtained ambiguous results, showing that the volume of new bone increased proportionally to the interconnection size. However, significant differences between groups based on the interconnection size were only observed at week 24. The pore size did not significantly affect osteoid matrix formation, except during the first 4 weeks, when greater new bone formation was observed in matrices with smaller pore sizes. At the same time, the authors found that a larger interconnection size contributes to new bone formation and recommended a minimum interconnection size of 120 μm [142]. On the other hand, Shor et al. showed that smaller pores (450 μm) had lower permeability compared to matrices with larger pores (750 μm), which allowed for better penetration of cell suspension into the matrix and cell adhesion [143]. Matrices with larger pores or higher porosity promoted cell viability and proliferation by preventing pore clogging and facilitating better penetration of nutrients and oxygen [144]. Although by now it has been recognized that larger pores in matrices of various origins contribute to better bone regeneration and revascularization, there are several studies indicating a limited role of pore size in osteointegration when using matrices with pore sizes ranging from 350 to 800 μm and porosity from 30% to 70% [145,146]. Based on conducted research, a critical pore size of 200 μm was determined, below which osteoblasts bridged the pore surface without any growth in the pores [140]. Fukuda et al. [147] studied osteoinduction of SLM Ti implants with a canal structure and observed pronounced osteoinduction with pore sizes of 500 and 600 μm. Wauthle et al. [148] investigated SLM tetrahedral porous Ta implants with an average pore size of 500 μm and 80% porosity, finding good in vivo biocompatibility of the implants. Wally et al. [149] analyzed the role of pore size in the porous structure of SLM Ti6Al4V, but were unable to draw a definitive conclusion due to the lack of correlation between pore structure and osseointegration.

Taniguchi et al. [150] reported that the SLM porous Ti6Al4V implant with a porosity of 65% and a pore size of 600 μm had comparable mechanical strength to bone, higher fixation capability, and greater bone ingrowth compared to implants with pore sizes of 300 and 900 μm. Wieding et al. [151] concluded that a porous Ti6Al4V matrix with a pore size of 700 μm stabilized segmental bone defects in sheep tarsal bones. Li et al. [152] and Chang et al. [139] conducted in vitro experiments to investigate matrices with pore sizes of 500 μm, 600 μm, and 700 μm, and porosities of 60% and 70%. Matrix with a size of 500 μm and a porosity of 60% demonstrated superior cell proliferation and osteogenic differentiation of rat bone marrow mesenchymal stem cells (MSCs) in vitro and bone ingrowth in vivo [153]. Liang et al. [118] studied titanium SLM implants with a porosity of 60-70%, which matched the mechanical characteristics of trabecular bone. This study found that a Ti matrix with a porosity of 70% and pore sizes of 313 μm and 390 μm promoted cell proliferation and bone ingrowth. It is hypothesized that not only the size, but also the combination of small and large pores,

Preprints (www.preprints.org) | NOT PEER-REVIEWED | Posted: 30 August 2023 doi:10.20944/preprints202308.1983.v1

plays an important role in cell colonization and proliferation within the matrix. In support of this idea it has been found that trabecular-like porous scaffolds with full irregularity and higher porosity promote the proliferation and differentiation of osteoblasts due to the combination of small and large pores of various shapes (0-1800 μm) and a roughness of 0.25 and 0.5 [118p7]. While increasing the pore size of matrices is believed to enhance osteointegration, the pore size has limited influence on bone ingrowth in later stages.

Some studies suggest that pores larger than 1 mm in diameter may promote the formation of fibrous tissue [135]. Despite a number of studies, the optimal porosity and pore size of bone ingrowth implants, especially porous SLM implants, are still insufficiently understood. Systematic investigation of the impact of porosity and pore size of porous SLM frameworks on mechanical and biological properties is crucial to enhance the reliability and safety of porous SLM frameworks for medical purposes. It is evident that, in addition to pore size, their geometry is also important for osteoinduction. Specifically, structures such as diamond and rhombic dodecahedron are optimal for elastic modulus and provide osteogenic metal matrices. Therefore, a porous Ti6Al4V framework with a rhombic dodecahedron as its elementary cell has the highest mechanical strength and moderate osteogenic properties, while a tantalum matrix with a diamond unit cell structure exhibits excellent osteogenic effects and moderate mechanical strength [154]. However, Lee et al. [155], while studying Ti-6Al-4V samples with pores of different shapes (round, triangular, and rectangular), concluded that the determining factor is not the shape but the pore topography. Therefore, it is necessary to evaluate the curvature and roughness of the surface, as samples with different pore shapes may have different surface topographies.

The analysis conducted allows us to conclude that despite a large number of studies conducted, optimal sizes and microarchitecture of matrix pores for bone tissue defect replacement have not yet been determined. The only indisputable fact is that these structures should be comparable to native bone in terms of mechanical properties, pore size, and geometry, providing adhesion, proliferation, and differentiation of osteoblast precursor cells.

5.3. Biocoatings of porous structures

Orthobiologicals are biological substances such as bioactive molecules, stem cells, or demineralized bone grafts that are used to heal bone defects more quickly. Porous matrices made of titanium alloy, printed on a 3D printer, enhance angiogenesis, osteoblast adhesion, and promote osseointegration. However, titanium alloys are biologically inert, making the attachment between the implant and bone tissue weak. Therefore, surface treatment and implant structure must be considered in order to develop optimal porous implants. Cell differentiation and bone ingrowth are accelerated when the implant surface is covered with a bioactive material or when chemical and thermal treatments are applied, transforming the smooth titanium surface into a rough bioactive surface [156]. It has been demonstrated that chemical and thermal treatment, by immersion in a 5M aqueous solution of NaOH at 60°C for 24 hours, enhances the osteoinductive properties of porous titanium implants and does not require additional use of osteogenic cells or bone morphogenetic protein. Thus, bioactive porous titanium could be an attractive alternative to existing orthopedic implants under load conditions [157]. There are several methods to enhance the biological activity of metallic implants through surface treatment with bioinert metals, simulated body fluid (SBF), which mimics the composition of human plasma. As a result, a biomimetic apatite coating can form on the material surface. One of them is plasma spraying of calcium phosphate, which is one of the most studied methods and its effectiveness has been confirmed [158]. Another method is biomimetic coating, where a bone-like apatite layer is created by immersing the metallic matrix in simulated body fluid (SBF) (Hanks's solution) [159,160]. Kon et al. applied dual-doped hydroxyapatite ($Ce4+/Si4+$ doped HAP) coating using centrifugation with extreme centrifugal force, which showed excellent biocompatibility with osteoblast cell line and antibacterial activity [161]. Like the embryonic development of bone, the healing of fractures is directly regulated by key cytokines such as bone morphogenetic proteins (BMPs), transforming growth factor-beta (TGF-β), FGF, parathyroid hormone (PTH), platelet-derived growth factors (PDGF), and the insulin-like growth factor 1 (IGF-1)

 doi:10.20944/preprints202308.1983.v1

family [162]. During the cascade of fracture healing, TGF-β and BMP are secreted, facilitating the recruitment of precursor cells, while FGF, PDGF, and IGF induce proliferation, and cellular differentiation is largely regulated by BMP [163–165]. As one of the main factors promoting bone tissue regeneration and approved for clinical use, BMP-2 has been utilized in clinical practice for the treatment of spinal fusion. BMP-2 is currently administered locally in the form of a soaked collagen sponge or allografts [166,167]. It has also been shown that systemic administration of recombinant BMP-2, BMP-6, or BMP-7 contributes to bone mass restoration [168–170]. Preclinical and clinical studies have shown that local application of recombinant human bone morphogenetic protein-2 (rhBMP-2) can promote bone tissue restoration in cases of bone defects, non-union fractures, spinal fusion, etc. [171,172]. An optimally balanced osteointegrative effect was observed with a concentration of BMP-2 at a dose of 100 μg/g coating. Bone formation during the first 3 weeks was moderate but still higher than in the control, and the process remained at a higher level for 3-6 weeks compared to lower drug concentrations [173]. The osteointegrative activity of BMP-2 is often overshadowed by severe adverse effects that can significantly impair the health and function of the patient's musculoskeletal system [174,175]. These include ectopic bone formation, paralysis, and neurological disorders [176,177]. It is known that many growth factors, including BMP-2, act pleiotropically. The initiation of a specific polarized effect largely depends on the concentration of the bioactive substance. However, the induced response can be easily reversed by secondary dosage adjustment. BMP-2 acts osteoinductive at low concentrations (from ng to μg) [178] and osteolytic at high concentrations in the mg range [179]. Various methods of applying BMP to the surface of metallic implants have been proposed to enhance their osteoinductivity. Lin et al. Used bioactive peptides isolated from mussels, including adhesion peptide-DOPA, anchoring peptide-RGD, and osteogenic-inducing peptide-BMP-2, as coatings on porous titanium alloy scaffolds printed on a 3D printer. In a rabbit model of bone defect, it was found that the implanted scaffolds with the bioactive coating stimulated osteointegration and exhibited mechanical stability [180]. However, simple application of bioactive peptides onto metallic surfaces allows for only a small amount to be adsorbed, and due to the low affinity of the protein to metallic surfaces, rapid release and penetration into the systemic circulation are observed. To successfully stimulate osteoinduction, large amounts of rhBMP-2 (up to 1.50 mg/ml) are required [181]. However, rapid release of high doses of bioactive peptides from the matrix increases the risk of complications, including ectopic bone formation, antibody formation against BMP, excessive bone resorption, and possibly the development of oncological diseases [182]. Therefore, biomimetic coatings saturated with BMP-2 have been used in studies with porous titanium. For this purpose, hydroxyapatite (HA), synthetic and natural polymer films are used. These strategies are mainly aimed at maintaining an effective local concentration of BMP for a longer period [183]. One possible way to ensure the long-term presence of BMP at the healing site is transfection of host cells at the site of injury with hBMP-2 DNA, resulting in their secretion of hBMP-2 protein at the healing site for many days [184–186]. The use of biomimetic coatings will undoubtedly increase biocompatibility and improve the osteointegration of porous titanium matrices, but for the successful application of these technologies, methods need to be developed that promote controlled local release of bioactive molecules, promoting proliferation of precursor cells without significant systemic and local adverse effects.

5.4. Cell colonization

For the purposes of bone tissue engineering, mesenchymal stem cells (MSCs) are widely used due to their ability to proliferate and undergo osteogenic differentiation [187]. Titanium possesses stable biocompatibility and, according to some studies, even promotes cell adhesion and proliferation [188] (Figure 3) In in vitro studies, titanium mesh membranes with square openings ranging from 25 μm to 75 μm have been shown to promote cell adhesion and proliferation [189]. Functionalizing titanium through the application of bioactive coatings, particularly derivatives of hydroxyapatite, significantly enhances MSC osteogenic differentiation and angiogenesis in human umbilical vein endothelial cells [190]. Endothelial microvascular network plays an important role in osteogenesis, bone regeneration, and bone tissue engineering. Endothelial progenitor cells (EPCs) have a high

Preprints (www.preprints.org) | NOT PEER-REVIEWED | Posted: 30 August 2023 doi:10.20944/preprints202308.1983.v1

angiogenic and vasculogenic potential. Colonization of EPC matrices enhances their vascularization and formation of new bone tissue. Additionally, EPCs enhance osteogenic differentiation and osteogenesis of MSCs [191]. However, co-implantation of MSCs and EPCs did not enhance matrix vascularization, presumably because MSCs themselves can stimulate angiogenesis [192,193]. The use of precursor cells with osteogenic and vasculogenic potential for populating matrices used in orthopedics is a promising direction. However, the limited number of studies in this area and the conflicting data obtained do not allow for a definitive determination of the role and significance of cellular technologies in creating bioimplants for bone defect replacement.

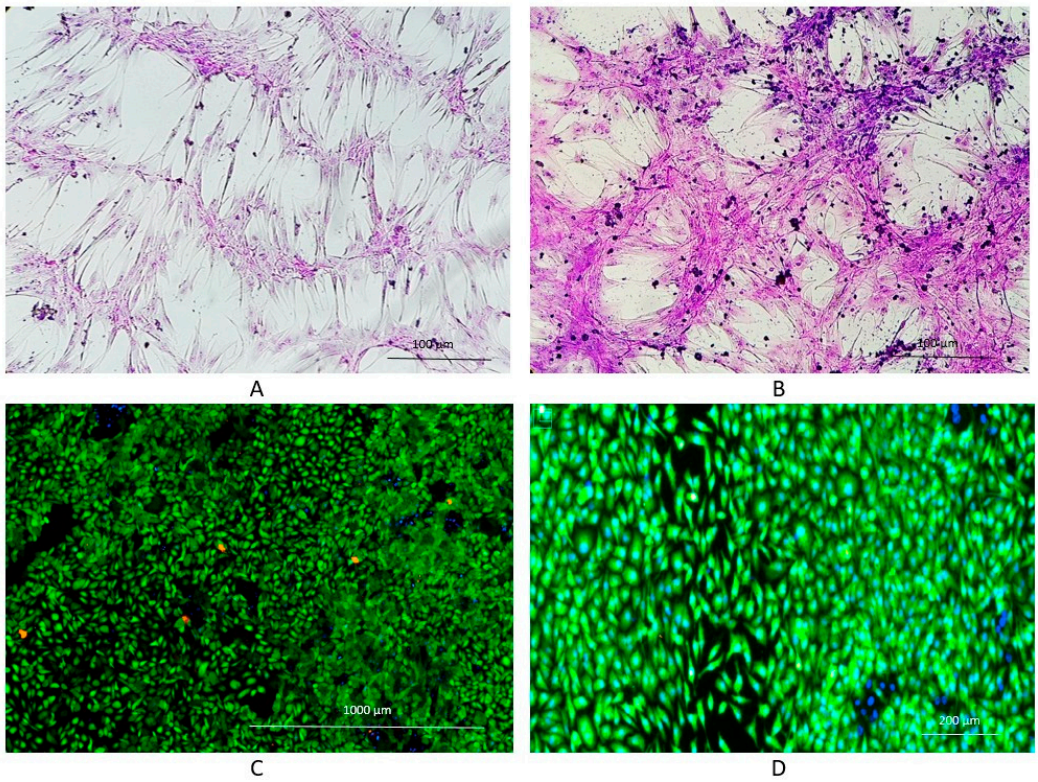

Figure 3. Proliferation of MSCs on plastic and titanium substrates in vitro. Proliferation of MSCs on plastic substrate original magnification 100 (A) and 400 (B), hematoxylin-eosin staining); Proliferation of MSCs on titanium substrate original magnification 100 (A) and 400 (B), green color – live cells Calcein AM staining, blue color – cell nuclei DAPI staining, red color– dead cells, propidium iodide staining (own unpublished data).

5.5. Clinical studies of porous T-based materials

In a clinical study, a porous titanium interbody cage was used in patients undergoing anterior cervical discectomy to achieve interbody fusion. The titanium cages were characterized by high porosity (80%) and large pore size (700 microns) to facilitate osteointegration. The results showed that the clinical effectiveness of the titanium cages was not significantly different from that of traditionally used polyetheretherketone with (auto) graft. However, faster consolidation was observed [194]. A more recent similar study on posterior lumbar interbody fusion using polyetheretherketone cages also did not reveal significant differences between the porous titanium cages and polyetheretherketone. However, it was suggested that porous titanium cages may reduce vertebral body subsidence and accelerate intervertebral fusion [195].

To achieve fusion in patients undergoing anterior cervical discectomy, 3D printed porous titanium and polyetheretherketone interbody cages with autograft were used as cervical implants. 3D printed porous titanium cervical implants demonstrated significantly better clinical outcomes. Although there were no differences between the groups after 12 months, the titanium cages led to faster vertebral consolidation [196]. In a clinical study, 51 patients with primary osteoarthritis of the

Preprints (www.preprints.org) | NOT PEER-REVIEWED | Posted: 30 August 2023 doi:10.20944/preprints202308.1983.v1

hip joint were randomized into two groups. In the experimental group, a porous titanium construct backside was implanted, while in the control group, patients were given a conventional porous coated titanium cup. When assessing periacetabular bone mineral density two years after surgery and implant fixation, no significant differences were observed between the two groups [197]. Similar data were obtained in another clinical study involving 248 patients with total hip arthroplasty. The authors compared the clinical and radiological outcomes between the conventional Stryker Trident HA cup and the high-porosity titanium cup. Both options showed good clinical results, however, the porous titanium led to a significantly higher rate of radiolucent lines around the cups, which was considered an indicator of possible cup loosening [198]. The described clinical studies indicate the promising potential of porous titanium scaffolds, which have comparable clinical effectiveness to standard materials and, unlike polyetheretherketone, do not require the additional use of autologous bone when used with cages. The increasing interest in 3D printed porous titanium in recent years is evident by the growing number of clinical trials registered on the website www.clinicaltrials.gov..

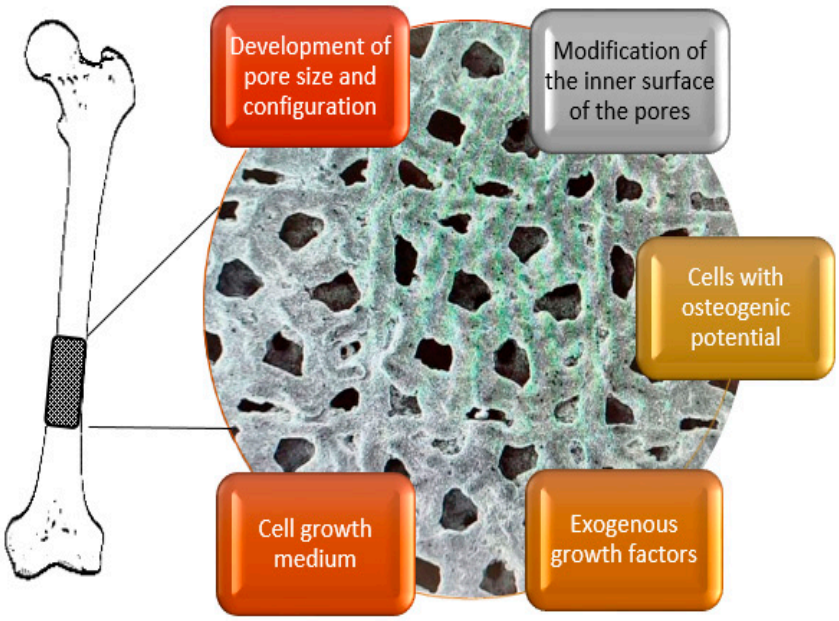

Figure 4. Algorithm for the development of an osteoconstructive porous Ti bioimplant.

6. Conclusions

A review of recent advances in the design of porous materials for the production of bioactive scaffolds by additive printing methods shows that such methods as selective laser fusion allow for the precise production of porous titanium alloys with adjustable cell geometry. Model methods of cell design (pore geometry, internal volume, pore/wall ratio, etc.) in combination with finite-element numerical calculations make it possible to calculate porous structures with adjustable elastic, strength and fatigue properties. Despite a number of current challenges such as residual powder removal, matching of designed and printed structures, the need for post-processing, etc., there are still a number of challenges to overcome. In addition, there are a number of unresolved biomedical issues that hinder the active introduction of a new generation of bioactive porous titanium scaffolds into clinical practice. This area looks extremely attractive from the point of view of creating advanced bioactive implants for the treatment of orthopaedic goals, including onco-orthopaedics.

Author Contributions: Conceptualization, M.V.K, N.Yu.A and N.A.E.; methodology, A.V.K. and A.A.R.; software, A.V.K. and D.N.K; formal analysis, M.V.K, N.Yu.A and N.A.E.; resources, V.V.P.; data curation, A.V.K.; writing—original draft preparation, M.V.K., N.Yu.A. and N.A.E.; writing—review and editing, M.V.K., N.Yu.A., A.A.R., A.V.K., D.N.K., V.V.P. and N.A.E.; visualization, A.V.K. and N.Yu.A.; supervision, M.V.K. and

N.A.E.; project administration, N.A.E.; funding acquisition, N.A.E. All authors have read and agreed to the published version of the manuscript.

Funding: This research was supported by Russian Science Foundation under grant #23-69-10003.

Institutional Review Board Statement: Ethical review and approval are waived for this work since it presents a review based on the published literature data.

Data Availability Statement: The data presented in this study are available on request from the corresponding author.

Conflicts of Interest: The authors declare no conflict of interest.

References

1. Davoodi, E.; Montazerian, H.; Mirhakimi, A.S.; Zhianmanesh, M.; Ibhadode, O.; Shahabad, S.I.; Esmaeilizadeh, R.; Sarikhanig, E.; Toorandaz, S.; Sarabi, S.A.; Nasiri, R.; Zhu, Y.; Kadkhodapour, J.; Li, B.; Khademhosseini, A.; Toyserkani, E. Additively manufactured metallic biomaterials. *Bioactive Mater.* **2022,** *15*, 214–249. https://doi.org/10.1016/j.bioactmat.2021.12.027
2. Vesvoranan, O.; Anup, A.; Hixon, K.R. Current Concepts and Methods in Tissue Interface Scaffold Fabrication. *Biomimetics* **2022**, *7*, 151. https://doi.org/10.3390/biomimetics7040151
3. Lv, Y; Wang, B; Liu, G; Tang, Y; Lu, E; Xie, K; Lan, C; Liu, J; Qin, Z; Wang, L. Metal Material, Properties and Design Methods of Porous Biomedical Scaffolds for Additive Manufacturing: A Review. *Front. Bioeng. Biotechnol*. **2021,** *9*, 641130. https://doi.org/10.3389/fbioe.2021.641130
4. Koju, N.; Niraula, S.; Fotovvati, B. Additively Manufactured Porous Ti6Al4V for Bone Implants: A Review. *Metals* **2022**, *12*, 687. https://doi.org/10.3390/met12040687
5. du Plessis, A.; Razavi, S.M.J.; Benedetti, M.; Murchio, S.; Leary, M.; Watson, M.; Bhate, D.; Berto, F. Properties and applications of additively manufactured metallic cellular materials: A review. *Prog. Mater. Sci.* **2022**, *125*, 100918. https://doi.org/10.1016/j.pmatsci.2021.100918
6. Marsell, R.; Einhorn, T. A. The Biology of Fracture Healing. *Injury* **2011**, *42*, 551–555. https://doi.org/10.1016%2Fj.injury.2011.03.031
7. Ho-Shui-Ling, A.; Bolander, J.; Rustom, L. E.; Johnson, A. W.; Luyten, F. P.; Picart, C. Bone regeneration strategies: Engineered scaffolds, bioactive molecules and stem cells current stage and future perspectives. *Biomaterials* **2018**, *180*, 143–162. https://doi.org/10.1016/j.biomaterials.2018.07.017
8. Newman, H.; Shih, Y. V.; Varghese, S. Resolution of inflammation in bone regeneration: From understandings to therapeutic applications. *Biomaterials* **2021**, *277*, 121114. https://doi.org/10.1016/j.biomaterials.2021.121114
9. The orthopaedic industry annual report 2023. Available online: https://www.orthoworld.com/the-orthopaedic-industry-annual-report/ (accessed on 23 August 2023)
10. de Villiers, T.J.; Goldstein, S.R. Bone Health 2022: An Update. *Climacteric* **2022**, *25*, 1–3. https://doi.org/10.1080/13697137.2021.1965408
11. Wu, Ai-Min et al. Global, regional, and national burden of bone fractures in 204 countries and territories, 1990–2019: a systematic analysis from the Global Burden of Disease Study 2019, *Lancet Healthy Longev*. **2021**, *2*, e580-e592. https://doi.org/10.1016/S2666-7568(21)00172-0
12. Brown, H.K.; Schiavone, K.; Gouin, F.; Heymann, M.F.; Heymann, D. Biology of Bone Sarcomas and New Therapeutic Developments. *Calcif Tissue Int*. **2018,** *102*, 174-195. https://doi.org/10.1007/s00223-017-0372-2
13. Thanindratarn, P; Dean, D.C.; Nelson, S.D.; Hornicek, F.J.; Duan, Z. Advances in immune checkpoint inhibitors for bone sarcoma therapy. *J. Bone Oncol.* **2019**, *15*, 100221. https://doi.org/10.1016/j.jbo.2019.100221
14. Ma, X.; Gao, Y.; Zhao, D.; Zhang, W.; Zhao, W.; Wu, M.; Cui, Y.; Li, Q.; Zhang, Z.; Ma, C. Titanium Implants and Local Drug Delivery Systems Become Mutual Promoters in Orthopedic Clinics. *Nanomaterials* **2022**, *12*, 47. https://doi.org/10.3390/nano12010047
15. Massaro, C.; Rotolo, P.; De Riccardis, F.; Milella, E.; Napoli, A.; Wieland, M.; Textor, M.; Spencer, N. D.; Brunette, D. M. Comparative investigation of the surface properties of commercial titanium dental implants. Part I: chemical composition. *J. Mater. Sci. Mater. Med.* **2002**, *13*, 535–548. https://doi.org/10.1023/A:1015170625506
16. Dutta, B.; Froes, F. H. (Sam) The Additive Manufacturing (AM) of Titanium Alloys. *Met. Powder Rep.* **2017**, *72*, 96–106. https://doi.org/10.1016/j.mprp.2016.12.062
17. Antunes, L. H. M.; de Lima, C. R. P. Cobalt-chromium alloys – properties and applications. *Reference Module in Materials Science and Materials Engineering* **2018**. https://doi.org/10.1016/B978-0-12-803581-8.09386-3
18. Goharian, A. Further development of trauma plating fixation. *Trauma Plating Systems* ed. by A. Goharian, Elsevier, **2017**, 361–381. https://doi.org/10.1016/B978-0-12-804634-0.00016-1
19. Zysset, P. K.; Edward Guo, X.; Edward Hoffler, C.; Moore, K. E.; Goldstein, S. A. Elastic modulus and hardness of cortical and trabecular bone lamellae measured by nanoindentation in the human femur. *J. Biomech.* **1999**, *32*, 1005–1012. https://doi.org/10.1016/S0021-9290(99)00111-6

20. Savio, D.; Bagno, A. When the total hip replacement fails: A review on the stress-shielding effect. *Processes* **2022**, *10*, 612. https://doi.org/10.3390/pr10030612
21. Kim, T.; See, C.W.; Li, X.; Zhu, D. Orthopedic implants and devices for bone fractures and defects: Past, present and perspective. *Eng. Regen.* **2020**, *1*, 6–18 https://doi.org/10.1016/j.engreg.2020.05.003
22. Derome, P.; Sternheim, A.; Backstein, D.; Malo, M. Treatment of large bone defects with trabecular metal cones in revision total Knee Arthroplasty. *J. Arthroplasty* **2014**, *29*, 122–126. https://doi.org/10.1016/j.arth.2013.04.033
23. Li, Y.; Yang, C.; Zhao, H.; Qu, S.; Li, X.; Li, Y. New developments of Ti-based alloys for biomedical applications. *Materials* **2014**, *7*, 1709–1800. https://doi.org/10.3390/ma7031709
24. Coffigniez, M.; Gremillard, L.; Balvay, S.; Lachambre, J.; Adrien, J.; Boulnat, X. Direct-ink writing of strong and biocompatible titanium scaffolds with bimodal interconnected porosity. *Addit. Manuf.* **2021**, *39*, 101859. https://doi.org/10.1016/j.addma.2021.101859
25. Kumar, P.; Ramamurty, U. Microstructural optimization through heat treatment for enhancing the fracture toughness and fatigue crack growth resistance of selective laser melted Ti-6Al-4V alloy. *Acta Mater.* **2019**, *169*, 45–59. https://doi.org/10.1016/j.actamat.2019.03.003
26. Renner, P.; Jha, S.; Chen, Y.; Raut, A.; Mehta, S. G.; Liang, H. A review on corrosion and wear of additively manufactured alloys. *J. Tribol.* **2021**, *143*. 050802. https://doi.org/10.1115/1.4050503
27. Pattanayak, D. K.; Fukuda, A.; Matsushita, T.; Takemoto, M.; Fujibayashi, S.; Sasaki, K.; Nishida, N.; Nakamura, T.; Kokubo, T. Bioactive Ti metal analogous to human cancellous bone: Fabrication by selective laser melting and chemical treatments. *Acta Biomater.* **2011**, *7*, 1398–1406. https://doi.org/10.1016/j.actbio.2010.09.034
28. Taniguchi, N.; Fujibayashi, S.; Takemoto, M.; Sasaki, K.; Otsuki, B.; Nakamura, T.; Matsushita, T.; Kokubo, T.; Matsuda, S. Effect of pore size on bone ingrowth into porous titanium implants fabricated by additive manufacturing: an in vivo experiment. *Mater. Sci. Eng. C* **2016**, *59*, 690–701. https://doi.org/10.1016/j.msec.2015.10.069
29. Davoodi, E.; Zhianmanesh, M.; Montazerian, H.; Milani, A. S.; Hoorfar, M. Nano-porous anodic alumina: Fundamentals and applications in tissue engineering. *J. Mater. Sci. Mater. Med.* **2020**, *31*, 60. https://doi.org/10.1007/s10856-020-06398-2
30. Al-Tamimi, A. A.; Peach, C.; Fernandes, P. R.; Cseke, A.; Bartolo, P. J. D. S. Topology optimization to reduce the stress shielding effect for orthopedic applications. *Procedia CIRP* **2017**, *65*, 202–206. https://doi.org/10.1016/j.procir.2017.04.032
31. Rahbari, A.; Montazerian, H.; Davoodi, E.; Homayoonfar, S. Predicting permeability of regular tissue engineering scaffolds: Scaling analysis of pore architecture, scaffold length, and fluid flow rate effects. *Comput. Methods Biomech. Biomed. Eng.* **2016**, *20*, 231–241. https://doi.org/10.1080/10255842.2016.1215436
32. Zhianmanesh, M.; Varmazyar, M.; Montazerian, H. Fluid permeability of graded porosity scaffolds architectured with minimal surfaces. *ACS Biomater. Sci. Eng.* **2019**, *5*, 1228–1237. https://doi.org/10.1021/acsbiomaterials.8b01400
33. Kim, F. H.; Moylan, S. P. *Literature review of Metal Additive Manufacturing Defects* **2018**. Advanced Manufacturing Series (NIST AMS), National Institute of Standards and Technology, Gaithersburg, MD, [online], https://doi.org/10.6028/NIST.AMS.100-16 (Accessed 23 August 2023)
34. Li, X.; Jia, X.; Yang, Q.; Lee, J. Quality Analysis in metal additive manufacturing with Deep Learning. *J. Intell. Manuf.* **2020**, *31*, 2003–2017. https://doi.org/10.1007/s10845-020-01549-2
35. Cui, W.; Zhang, Y.; Zhang, X.; Li, L.; Liou, F. Metal additive manufacturing parts inspection using convolutional neural network. *Appl. Sci.* **2020**, *10*, 545. https://doi.org/10.3390/app10020545
36. Mellor, S.; Hao, L.; Zhang, D. Additive manufacturing: A framework for implementation. *Int. J. Prod. Econ.* **2014**, *149*, 194–201. https://doi.org/10.1016/j.ijpe.2013.07.008
37. Mondal, P.; Wazeer, A.; Das, A.; Karmakar, A. Low cost porous Ti-6Al-4 V structures by additive manufacturing for orthopaedic applications. *Mater. Today Proc.* **2022**, *67*, 398–403. https://doi.org/10.1016/j.matpr.2022.07.349
38. Xiong, Y.; Han, Z.; Qin, J.; Dong, L.; Zhang, H.; Wang, Y.; Chen, H.; Li, X. Effects of porosity gradient pattern on mechanical performance of additive manufactured Ti-6Al-4V functionally graded porous structure. *Mater. Des.* **2021**, *208*, 109911. https://doi.org/10.1016/j.matdes.2021.109911
39. Awad, A.; Fina, F.; Goyanes, A.; Gaisford, S.; Basit, A. W. 3D printing: Principles and pharmaceutical applications of Selective Laser Sintering. *Int. J. Pharm.* **2020**, *586*, 119594. https://doi.org/10.1016/j.ijpharm.2020.119594
40. Herzog, D.; Seyda, V.; Wycisk, E.; Emmelmann, C. Additive Manufacturing of Metals. *Acta Mater.* **2016**, *117*, 371–392. https://doi.org/10.1016/j.actamat.2016.07.019
41. Ataee, A.; Li, Y.; Wen, C. A comparative study on the nanoindentation behavior, wear resistance and in vitro biocompatibility of SLM manufactured CP–TI and EBM manufactured TI64 gyroid scaffolds. *Acta Biomater.* **2019**, *97*, 587–596. https://doi.org/10.1016/j.actbio.2019.08.008

42. Murr, L. E. Metallurgy principles applied to powder bed fusion 3D printing/additive manufacturing of personalized and optimized metal and alloy biomedical implants: An overview. *J Mater. Res. Technol.* **2020**, *9*, 1087–1103. https://doi.org/10.1016/j.jmrt.2019.12.015
43. Gu, D.; Shi, X.; Poprawe, R.; Bourell, D.L.; Setchi, R.; Zhu, J. Material-structure-performance integrated laser-metal additive manufacturing. *Science* **2021,** *372*, eabg1487 **2023**, 1–33. https://doi.org/10.1126/science.abg1487
44. Dumpa, N.; Butreddy, A.; Wang, H.; Komanduri, N.; Bandari, S.; Repka, M. A. 3D printing in Personalized Drug Delivery: An overview of hot-melt extrusion-based fused deposition modeling. *Int. J. Pharm.* **2021**, *600*, 120501. https://doi.org/10.1016/j.ijpharm.2021.120501
45. Kumar, V.; Kaur, H.; Kumari, A.; Hooda, G.; Garg, V.; Dureja, H. Drug delivery and testing via 3D printing. *Bioprinting* **2023,** e00298. https://doi.org/10.1016/j.bprint.2023.e00298
46. Jiao, Y.; Li, X.; Zhang, X.; Li, G.; Fang, J.; Xuan, S.; Liu, L.; Wang, S.; Xie, H. Silver antibacterial surface adjusted by hierarchical structure on 3D printed porous titanium alloy. *Appl. Surf. Sci.* **2023**, *610*, 155519. https://doi.org/10.1016/j.apsusc.2022.155519
47. Tshephe, T. S.; Akinwamide, S. O.; Olevsky, E.; Olubambi, P. A. Additive manufacturing of titanium-based alloys- a review of methods, properties, challenges, and prospects. *Heliyon* **2022**, *8*, e09041. https://doi.org/10.1016/j.heliyon.2022.e09041
48. Farazin, A.; Zhang, C.; Gheisizadeh, A.; Shahbazi, A. 3D bio-printing for use as bone replacement tissues: A review of Biomedical Application. *Biomed. Eng. Adv.* **2023**, *5*, 100075. https://doi.org/10.1016/j.bea.2023.100075
49. Weaver, J. S.; Heigel, J. C.; Lane, B. M. Laser spot size and scaling laws for laser beam additive manufacturing. *J. Manuf. Processes* **2022**, *73*, 26–39. https://doi.org/10.1016/j.jmapro.2021.10.053
50. Dutta, B.; Froes, F. H. (Sam) The Additive Manufacturing (AM) of Titanium Alloys. *Met. Powder Rep.* **2017**, *72*, 96–106. https://doi.org/10.1016/j.mprp.2016.12.062
51. Keaveney, S.; Shmeliov, A.; Nicolosi, V.; Dowling, D. P. Investigation of process by-products during the selective laser melting of Ti6Al4V powder. *Additive Manufacturing* **2020**, *36*, 101514. https://doi.org/10.1016/j.addma.2020.101514
52. Dowling, L.; Kennedy, J.; O'Shaughnessy, S.; Trimble, D. A review of critical repeatability and reproducibility issues in powder bed fusion. *Materials and Design* **2020**, *186*, 108346. https://doi.org/10.1016/j.matdes.2019.108346
53. Guo, A. X. Y.; Cheng, L.; Zhan, S.; Zhang, S.; Xiong, W.; Wang, Z.; Wang, G.; Cao, S. C. Biomedical applications of the powder-based 3D Printed Titanium Alloys: A Review. *Journal of Materials Science and Technology* **2022**, *125*, 252–264. https://doi.org/10.1016/j.jmst.2021.11.084
54. Ma, K.; Chen, H.; Shen, Y.; Guo, Y.; Li, W.; Wang, Y.; Zhang, Y.; Sun, Y. Feasibility Study and material selection for powder-bed fusion process in printing of Denture clasps. *Computers in Biology and Medicine* **2023**, *157*, 106772. https://doi.org/10.1016/j.compbiomed.2023.106772
55. Hwang, S.; An, S.; Robles, U.; Rumpf, R. C. Process parameter optimization for removable partial denture frameworks manufactured by Selective Laser Melting. *The Journal of Prosthetic Dentistry* **2023**, *129*, 191–198. https://doi.org/10.1016/j.prosdent.2021.04.021
56. Roberson, G. A.; Sinha, P. K. 3D printing in Orthodontics: A practical guide to the Printer Technology and selection. *Seminars in Orthodontics* **2022**, *28*, 100–106. https://doi.org/10.1053/j.sodo.2022.10.006
57. Gu, D.; Hagedorn, Y.C.; Meiners, W.; Meng, G.; Batista, R.J.S.; Wissenbach, K.; Poprawe, R. Densification behavior, microstructure evolution, and wear performance of selective laser melting processed commercially pure titanium. *Acta Mater.* **2012**, *60*, 3849-3860. https://doi.org/10.1016/j.actamat.2012.04.006
58. Barbas, A.; Bonnet, A.-S.; Lipinski, P.; Pesci, R.; Dubois, G. Development and mechanical characterization of porous titanium bone substitutes. *Journal of the Mechanical Behavior of Biomedical Materials* **2012**, *9*, 34–44. https://doi.org/10.1016/j.jmbbm.2012.01.008
59. Guo, S.; Li, Y.; Gu, J.; Liu, J.; Peng, Y.; Wang, P.; Zhou, Q.; Wang, K. Microstructure and mechanical properties of Ti6Al4V/ B4C titanium matrix composite fabricated by selective laser melting (SLM). *Journal of Materials Research and Technology* **2023**, *23*, 1934–1946. https://doi.org/10.3390/met13020264
60. d18 Xiao, Y. K.; Bian, Z. Y.; Wu, Y.; Ji, G.; Lian, Q.; Wang, H. Z.; Chen, Z.; Wang, H. W. Simultaneously minimizing residual stress and enhancing strength of selective laser melted nano-TiB2 decorated Al alloy via post-uphill quenching and ageing. *Mater. Charact.* **2021**, *178*, 111242. https://doi.org/10.1016/j.matchar.2021.111242
61. Thijs, L.; Verhaeghe, F.; Craeghs, T.; Humbeeck, J. V.; Kruth, J.-P. A study of the microstructural evolution during selective laser melting of ti–6al–4v. *Acta Materialia* **2010**, *58*, 3303–3312. https://doi.org/10.1016/j.actamat.2010.02.004
62. He, K.; Zhao, X. 3D thermal finite element analysis of the SLM 316L parts with microstructural correlations. *Complexity* **2018**, *2018*, 1–13. https://doi.org/10.1155/2018/6910187

63. Kruth, J. P.; Froyen, L.; Van Vaerenbergh, J.; Mercelis, P.; Rombouts, M.; Lauwers, B. Selective laser melting of iron-based powder. *Journal of Materials Processing Technology* **2004**, *149*, 616–622. https://doi.org/10.1016/j.jmatprotec.2003.11.051
64. Xu, W.; Brandt, M.; Sun, S.; Elambasseril, J.; Liu, Q.; Latham, K.; Xia, K.; Qian, M. Additive manufacturing of strong and ductile ti–6al–4v by selective laser melting via in situ martensite decomposition. *Acta Materialia* **2015**, *85*, 74–84. https://doi.org/10.1016/j.actamat.2014.11.028
65. Murr, L. E.; Quinones, S. A.; Gaytan, S. M.; Lopez, M. I.; Rodela, A.; Martinez, E. Y.; Hernandez, D. H.; Martinez, E.; Medina, F.; Wicker, R. B. Microstructure and mechanical behavior of ti–6al–4v produced by rapid-layer manufacturing, for biomedical applications. *Journal of the Mechanical Behavior of Biomedical Materials* **2009**, *2*, 20–32. https://doi.org/10.1016/j.jmbbm.2008.05.004
66. Wysocki, B.; Maj, P.; Krawczyńska, A.; Rożniatowski, K.; Zdunek, J.; Kurzydłowski, K. J.; Święszkowski, W. Microstructure and mechanical properties investigation of CP titanium processed by selective laser melting (SLM). *Journal of Materials Processing Technology* **2017**, *241*, 13–23. https://doi.org/10.1016/j.jmatprotec.2016.10.022
67. Kruth, J.; Mercelis, P.; Van Vaerenbergh, J.; Froyen, L.; Rombouts, M. Binding mechanisms in selective laser sintering and Selective Laser melting. *Rapid Prototyping Journal* **2005**, *11*, 26–36. https://doi.org/10.1108/13552540510573365
68. Jin, B.; Wang, Q.; Zhao, L.; Pan, A.; Ding, X.; Gao, W.; Song, Y.; Zhang, X. A Review of Additive Manufacturing Techniques and Post-Processing for High-Temperature Titanium Alloys. *Metals* **2023**, *13*, 1327. https://doi.org/10.3390/met13081327
69. Wei, J.; Sun, H.; Zhang, D.; Gong, L.; Lin, J.; Wen, C. Influence of heat treatments on microstructure and mechanical properties of TI–26NB alloy elaborated in situ by laser additive manufacturing with ti and NB mixed powder. *Materials* **2018**, *12*, 61. https://doi.org/10.3390/ma12010061
70. Vrancken, B.; Thijs, L.; Kruth, J.-P.; Van Humbeeck, J. Heat treatment of ti6al4v produced by selective laser melting: Microstructure and mechanical properties. *Journal of Alloys and Compounds* **2012**, *541*, 177–185. https://doi.org/10.1016/j.jallcom.2012.07.022
71. Barriobero-Vila, P.; Gussone, J.; Stark, A.; Requena, G.; Schell, N.; Haubrich, J. Peritectic Titanium Alloys for 3D Printing. *Nat. Commun.* **2018**, *9*, 3426. https://doi.org/10.1038/s41467-018-05819-9
72. Phani Babu, V. V.; GB, V. K. A review on 3D printing process on metals and their surface roughness and dimensional accuracy. *Materials Today: Proceedings* **2022**, *64*, 523–530. https://doi.org/10.1016/j.matpr.2022.05.018
73. Khrapov, D.; Paveleva, A.; Kozadayeva, M.; Evsevleev, S.; Mishurova, T.; Bruno, G.; Surmenev, R.; Koptyug, A.; Surmeneva, M. Trapped powder removal from sheet-based porous structures based on triply periodic minimal surfaces fabricated by electron beam powder bed fusion. *Materials Science and Engineering: A* **2023**, *862*, 144479. https://doi.org/10.1016/j.msea.2022.144479
74. Wang, S.; Ning, J.; Zhu, L.; Yang, Z.; Yan, W.; Dun, Y.; Xue, P.; Xu, P.; Bose, S.; Bandyopadhyay, A. Role of porosity defects in metal 3d printing: Formation Mechanisms, impacts on properties and mitigation strategies. *Materials Today* **2022**, *59*, 133–160. https://doi.org/10.1016/j.mattod.2022.08.014
75. Gibson, L. J.; Ashby, M. F.; Harley, B. A. *Cellular materials in nature and medicine*; Cambridge University Press: Cambridge, 2010.
76. Olivares, A. L.; Lacroix, D. Simulation of cell seeding within a three-dimensional porous scaffold: A fluid-particle analysis. *Tissue Engineering Part C: Methods* **2012**, *18*, 624–631. https://doi.org/10.1089/ten.tec.2011.0660
77. Rahbari, A.; Montazerian, H.; Davoodi, E.; Homayoonfar, S. Predicting permeability of regular tissue engineering scaffolds: Scaling analysis of pore architecture, scaffold length, and fluid flow rate effects. *Computer Methods in Biomechanics and Biomedical Engineering* **2016**, *20*, 231–241. https://doi.org/10.1080/10255842.2016.1215436
78. Castro, A. P.; Ruben, R. B.; Gonçalves, S. B.; Pinheiro, J.; Guedes, J. M.; Fernandes, P. R. Numerical and experimental evaluation of TPMS gyroid scaffolds for bone tissue engineering. *Comp. Meth. Biomech. Biomed. Eng.* **2019**, *22*, 567–573. https://doi.org/10.1080/10255842.2019.1569638
79. Castilho, M.; Pires, I.; Gouveia, B.; Rodrigues, J. Structural evaluation of scaffolds prototypes produced by three-dimensional printing. *The International Journal of Advanced Manufacturing Technology* **2011**, *56*, 561–569. https://doi.org/10.1007/s00170-011-3219-4
80. Papantoniou, I.; Guyot, Y.; Sonnaert, M.; Kerckhofs, G.; Luyten, F. P.; Geris, L.; Schrooten, J. Spatial optimization in perfusion bioreactors improves bone tissue-engineered construct quality attributes. *Biotechnology and Bioengineering* **2014**, *111*, 2560–2570. https://doi.org/10.1002/bit.25303
81. Bertassoni, L.E.; Coelho, P.G. Engineering mineralized and load bearing tissues; Springer: Cham, 2015. https://doi.org/10.1007/978-3-319-22345-2
82. Bobbert, F. S. L.; Lietaert, K.; Eftekhari, A. A.; Pouran, B.; Ahmadi, S. M.; Weinans, H.; Zadpoor, A. A. Additively manufactured metallic porous biomaterials based on minimal surfaces: A unique combination

of topological, mechanical, and mass transport properties. *Acta Biomaterialia* **2017**, *53*, 572–584. https://doi.org/10.1016/j.actbio.2017.02.024
83. Lu, T.; Li, Y.; Chen, T. Techniques for fabrication and construction of three-dimensional scaffolds for tissue engineering. *International Journal of Nanomedicine* **2013**, 337. https://doi.org/10.2147/IJN.S38635
84. Yoo, D.-J. Advanced porous scaffold design using multi-void triply periodic minimal surface models with high surface area to volume ratios. *International Journal of Precision Engineering and Manufacturing* **2014**, *15*, 1657–1666. https://doi.org/10.1007/s12541-014-0516-5
85. Shi, J.; Wei, F.; Chouraki, B.; Sun, X.; Wei, J.; Zhu, L. Study on Performance Simulation of Vascular-like Flow Channel Model Based on TPMS Structure. *Biomimetics* **2023**, *8*, 69. https://doi.org/10.3390/biomimetics8010069
86. Feng, J.; Fu, J.; Shang, C.; Lin, Z.; Li, B. Porous scaffold design by solid T-splines and triply periodic minimal surfaces. *Computer Methods in Applied Mechanics and Engineering* **2018**, *336*, 333–352. https://doi.org/10.1016/j.cma.2018.03.007
87. Al-Ketan, O.; Abu Al-Rub, R. K. Multifunctional mechanical metamaterials based on triply periodic minimal surface lattices. *Adv. Eng. Mater.* **2019**, *21*, 1900524. http://dx.doi.org/10.1002/adem.201900524
88. Liu, F.; Mao, Z.; Zhang, P.; Zhang, D. Z.; Jiang, J.; Ma, Z. Functionally graded porous scaffolds in multiple patterns: New design method, physical and mechanical properties. *Materials and Design* **2018**, *160*, 849–860. https://doi.org/10.1016/j.matdes.2018.09.053
89. Al-Ketan, O.; Abu Al-Rub, R. K. MSLattice: A free software for generating uniform and graded lattices based on triply periodic minimal surfaces. *Material Design and Processing Communications* **2020**, *3*, 6, 205. https://doi.org/10.1002/mdp2.205
90. Gabbrielli, R.; Turner, I. G.; Bowen, C. R. Development of modelling methods for materials to be used as bone substitutes. *Bioceramics 20* **2007**, 903–906. https://doi.org/10.4028/www.scientific.net/KEM.361-363.903
91. Baravalle, R.; Scandolo, L.; Delrieux, C.; García Bauza, C.; Eisemann, E. Realistic modeling of porous materials. *Comput Animat Virtual Worlds*. **2017,** *28*, e1719. https://doi.org/10.1002/cav.1719
92. Bermejillo Barrera, M.D.; Franco-Martínez, F.; Díaz Lantada, A. Artificial Intelligence Aided Design of Tissue Engineering Scaffolds Employing Virtual Tomography and 3D Convolutional Neural Networks. *Materials* **2021**, *14*, 5278. https://doi.org/10.3390/ma14185278
93. Merayo, D.; Rodriguez-Prieto, A.; Camacho, A. M. Prediction of physical and mechanical properties for metallic materials selection using big data and Artificial Neural Networks. *IEEE Access* **2020**, *8*, 13444–13456 https://doi.org/10.1109/ACCESS.2020.2965769
94. Javaid, S.; Gorji, H. T.; Soulami, K. B.; Kaabouch, N. Identification and ranking biomaterials for bone scaffolds using machine learning and PROMETHEE. *Res. Biomed. Eng.* **2023**, *39*, 129–138. https://doi.org/10.1007/s42600-022-00257-5
95. Jafari Chashmi, M.; Fathi, A.; Shirzad, M.; Jafari-Talookolaei, R.-A.; Bodaghi, M.; Rabiee, S. M. Design and analysis of porous functionally graded femoral prostheses with improved stress shielding. *Designs* **2020**, *4*, 12. https://doi.org/10.3390/designs4020012
96. Vora, L. K.; Gholap, A. D.; Jetha, K.; Thakur, R. R.; Solanki, H. K.; Chavda, V. P. Artificial Intelligence in pharmaceutical technology and Drug Delivery Design. *Pharmaceutics* **2023**, *15*, 1916. https://doi.org/10.3390/pharmaceutics15071916
97. Conev, A.; Litsa, E. E.; Perez, M. R.; Diba, M.; Mikos, A. G.; Kavraki, L. E. Machine learning-guided three-dimensional printing of tissue engineering scaffolds. *Tissue Eng. Part A* **2020**, *26*, 1359–1368. https://doi.org/10.1089/ten.TEA.2020.0191
98. Sujeeun, L. Y.; Goonoo, N.; Ramphul, H.; Chummun, I.; Gimié, F.; Baichoo, S.; Bhaw-Luximon, A. Correlating *in vitro* performance with physico-chemical characteristics of nanofibrous scaffolds for skin tissue engineering using supervised machine learning algorithms. *Royal Society Open Science* **2020**, *7*, 201293. https://doi.org/10.1098/rsos.201293
99. Zhou, J.; Xiong, S.; Liu, M.; Yang, H.; Wei, P.; Yi, F.; Ouyang, M.; Xi, H.; Long, Z.; Liu, Y.; Li, J.; Ding, L.; Xiong, L. Study on the influence of scaffold morphology and structure on osteogenic performance. *Front. Bioeng. Biotechnol.* **2023**, *11*, https://doi.org/10.3389/fbioe.2023.1127162
100. Quan, H.; Zhang, T.; Xu, H.; Luo, S.; Nie, J.; Zhu, X. Photo-curing 3D printing technique and its challenges. *Bioact. Mater.* **2020**, *5*, 110–115. https://doi.org/10.1016/j.bioactmat.2019.12.003
101. Lo Re, G.; Lopresti, F.; Petrucci, G.; Scaffaro, R. A facile method to determine pore size distribution in porous scaffold by using image processing. *Micron* **2015**, *76*, 37–45. https://doi.org/10.1016/j.micron.2015.05.001
102. Zhu, J.; Zou, S.; Mu, Y.; Wang, J.; Jin, Y. Additively manufactured scaffolds with optimized thickness based on triply periodic minimal surface. *Materials* **2022**, *15*, 7084. https://doi.org/10.3390/ma15207084
103. Ferracini, R.; Martínez Herreros, I.; Russo, A.; Casalini, T.; Rossi, F.; Perale, G. Scaffolds as structural tools for bone-targeted drug delivery. *Pharmaceutics* **2018**, *10*, 122. https://doi.org/10.3390/pharmaceutics10030122

104. Domsta, V.; Hänsch, C.; Lenz, S.; Gao, Z.; Matin-Mann, F.; Scheper, V.; Lenarz, T.; Seidlitz, A. The influence of shape parameters on unidirectional drug release from 3D printed implants and prediction of release from implants with individualized shapes. *Pharmaceutics* **2023**, *15*, 1276. https://doi.org/10.3390/pharmaceutics15041276
105. Zamoume, O.; Thibault, S.; Regnié, G.; Mecherri, M. O.; Fiallo, M.; Sharrock, P. Macroporous calcium phosphate ceramic implants for sustained drug delivery. *Mater. Sci. Eng. C* **2011**, *31*, 1352–1356. https://doi.org/10.1016/j.msec.2011.04.020
106. Roseti, L.; Parisi, V.; Petretta, M.; Cavallo, C.; Desando, G.; Bartolotti, I.; Grigolo, B. Scaffolds for bone tissue engineering: State of the art and new perspectives. *Materials Science and Engineering: C* **2017**, *78*, 1246–1262. https://doi.org/10.1016/j.msec.2017.05.017
107. Tang, D.; Tare, R. S.; Yang, L.-Y.; Williams, D. F.; Ou, K.-L.; Oreffo, R. O. C. Biofabrication of bone tissue: Approaches, challenges and translation for Bone Regeneration. *Biomaterials* **2016**, *83*, 363–382. https://doi.org/10.1016/j.biomaterials.2016.01.024
108. Li, J.; Chen, M.; Fan, X.; Zhou, H. Recent advances in bioprinting techniques: Approaches, applications and future prospects. *Journal of Translational Medicine* **2016**, *14* https://doi.org/10.1016/j.matdes.2023.111885
109. Aljohani, W.; Ullah, M. W.; Zhang, X.; Yang, G. Bioprinting and its applications in tissue engineering and Regenerative Medicine. *International Journal of Biological Macromolecules* **2018**, *107*, 261–275. https://doi.org/10.1016/j.ijbiomac.2017.08.171
110. Adepu, S.; Dhiman, N.; Laha, A.; Sharma, C. S.; Ramakrishna, S.; Khandelwal, M. Three-dimensional bioprinting for bone tissue regeneration. *Current Opinion in Biomedical Engineering* **2017**, *2*, 22–28. https://doi.org/10.1016/j.cobme.2017.03.005
111. Lin, K.-F.; He, S.; Song, Y.; Wang, C.-M.; Gao, Y.; Li, J.-Q.; Tang, P.; Wang, Z.; Bi, L.; Pei, G.-X. Low-temperature additive manufacturing of Biomimic three-dimensional hydroxyapatite/collagen scaffolds for bone regeneration. *ACS Applied Materials and Interfaces* **2016**, *8*, 6905–6916. https://doi.org/10.1021/acsami.6b00815
112. Park, J. Y.; Shim, J.-H.; Choi, S.-A.; Jang, J.; Kim, M.; Lee, S. H.; Cho, D.-W. 3D printing technology to control BMP-2 and VEGF delivery spatially and temporally to promote large-volume bone regeneration. *Journal of Materials Chemistry B* **2015**, *3*, 5415–5425. https://doi.org/10.1039/C5TB00637F
113. Ratheesh, G.; Venugopal, J. R.; Chinappan, A.; Ezhilarasu, H.; Sadiq, A.; Ramakrishna, S. 3D fabrication of polymeric scaffolds for regenerative therapy. *ACS Biomaterials Science and Engineering* **2017**, *3*, 1175–1194. https://doi.org/10.1021/acsbiomaterials.6b00370
114. Leong, K. F.; Cheah, C. M.; Chua, C. K. Solid freeform fabrication of three-dimensional scaffolds for engineering replacement tissues and organs. *Biomater.* **2003**, *24*, 2363–2378. https://doi.org/10.1016/S0142-9612(03)00030-9.
115. Kruth, J.-P.; Levy, G.; Klocke, F.; Childs, T. H. C. Consolidation phenomena in laser and powder-bed based layered manufacturing. *CIRP Annals* **2007**, *56*, 730–759. https://doi.org/10.1016/j.cirp.2007.10.004
116. Thijs, L.; Verhaeghe, F.; Craeghs, T.; Humbeeck, J. V.; Kruth, J.-P. A study of the microstructural evolution during selective laser melting of ti–6al–4v. *Acta Materialia* **2010**, *58*, 3303–3312. https://doi.org/10.1016/j.actamat.2010.02.004
117. Warnke, P. H.; Douglas, T.; Wollny, P.; Sherry, E.; Steiner, M.; Galonska, S.; Becker, S. T.; Springer, I. N.; Wiltfang, J.; Sivananthan, S. Rapid prototyping: Porous titanium alloy scaffolds produced by selective laser melting for bone tissue engineering. *Tissue Engineering Part C: Methods* **2009**, *15*, 115–124 http://doi.org/10.1089/ten.tec.2008.0288
118. Liang, H.; Yang, Y.; Xie, D.; Li, L.; Mao, N.; Wang, C.; Tian, Z.; Jiang, Q.; Shen, L. Trabecular-like Ti-6Al-4V scaffolds for orthopedic: Fabrication by selective laser melting and in vitro biocompatibility. *Journal of Materials Science and Technology* **2019**, *35*, 1284–1297. https://doi.org/10.1016/j.compositesb.2022.110057
119. Yang, Y.; Yuan, F.; Gao, C.; Feng, P.; Xue, L.; He, S.; Shuai, C. A combined strategy to enhance the properties of Zn by Laser Rapid Solidification and laser alloying. *Journal of the Mechanical Behavior of Biomedical Materials* **2018**, *82*, 51–60 https://doi.org/10.1016/j.jmbbm.2018.03.018
120. Giannitelli, S. M.; Accoto, D.; Trombetta, M.; Rainer, A. Current trends in the design of scaffolds for computer-aided tissue engineering. *Acta Biomaterialia* **2014**, *10*, 580–594. https://doi.org/10.1016/j.actbio.2013.10.024
121. Wang, X.; Xu, S.; Zhou, S.; Xu, W.; Leary, M.; Choong, P.; Qian, M.; Brandt, M.; Xie, Y. M. Topological design and additive manufacturing of porous metals for bone scaffolds and orthopaedic implants: A Review. *Biomaterials* **2016**, *83*, 127–141. https://doi.org/10.1016/j.biomaterials.2016.01.012
122. Van Bael, S.; Chai, Y. C.; Truscello, S.; Moesen, M.; Kerckhofs, G.; Van Oosterwyck, H.; Kruth, J.-P.; Schrooten, J. The effect of pore geometry on the in vitro biological behavior of human periosteum-derived cells seeded on selective laser-melted ti6al4v bone scaffolds. *Acta Biomater.* **2012**, *8*, 2824–2834. https://doi.org/10.1016/j.actbio.2012.04.001

123. Wang, Z.; Wang, C.; Li, C.; Qin, Y.; Zhong, L.; Chen, B.; Li, Z.; Liu, H.; Chang, F.; Wang, J. Analysis of factors influencing bone ingrowth into three-dimensional printed porous metal scaffolds: A Review. *Journal of Alloys and Compounds* **2017**, *717*, 271–285. https://doi.org/10.1016/j.jallcom.2017.05.079
124. Lv, X.; Wang, S.; Xu, Z.; Liu, X.; Liu, G.; Cao, F.; Ma, Y. Structural Mechanical Properties of 3D Printing Biomimetic Bone Replacement Materials. *Biomimetics* **2023**, *8*, 166. https://doi.org/10.3390/biomimetics8020166.
125. Cheng, A.; Humayun, A.; Cohen, D. J.; Boyan, B. D.; Schwartz, Z. Additively manufactured 3D porous ti-6al-4v constructs mimic trabecular bone structure and regulate osteoblast proliferation, differentiation and local factor production in a porosity and surface roughness dependent manner. *Biofabrication* **2014**, *6*, 045007 https://doi.org/10.1088/1758-5082/6/4/045007
126. Kou, X. Y.; Tan, S. T. A simple and effective geometric representation for irregular porous structure modeling. *Computer-Aided Design* **2010**, *42*, 930–941. https://doi.org/10.1016/j.cad.2010.06.006
127. Zhang, X.; Tang, L.; Liu, Z.; Jiang, Z.; Liu, Y.; Wu, Y. Yield properties of closed-cell aluminum foam under triaxial loadings by a 3D Voronoi model. *Mechanics of Materials* **2017**, *104*, 73–84. https://doi.org/10.1016/j.mechmat.2016.10.007
128. Honda, H.; Nagai, T. Cell models lead to understanding of multi-cellular morphogenesis consisting of successive self-construction of cells. *Journal of Biochemistry* **2014**, *157*, 129–136. https://doi.org/10.1093/jb/mvu088
129. Wang, G.; Shen, L.; Zhao, J.; Liang, H.; Xie, D.; Tian, Z.; Wang, C. Design and compressive behavior of controllable irregular porous scaffolds: Based on Voronoi-tessellation and for additive manufacturing. *ACS Biomater. Sci. Eng.* **2018**, *4*, 719–727. https://doi.org/10.1021/acsbiomaterials.7b00916
130. Fantini, M.; Curto, M.; De Crescenzio, F. A method to design biomimetic scaffolds for bone tissue engineering based on Voronoi lattices. *Virtual and Physical Prototyping* **2016**, *11*, 77–90. https://doi.org/10.1080/17452759.2016.1172301
131. Gómez, S.; Vlad, M. D.; López, J.; Fernández, E. Design and properties of 3D scaffolds for bone tissue engineering. *Acta Biomaterialia* **2016**, *42*, 341–350. https://doi.org/10.1016/j.actbio.2016.06.032
132. Costa, A. Permeability-porosity relationship: A reexamination of the kozeny-carman equation based on a fractal pore-space geometry assumption. *Geophysical Research Letters* **2006**, *33*. https://doi.org/10.1029/2005GL025134
133. Hulbert, S. F.; Young, F. A.; Mathews, R. S.; Klawitter, J. J.; Talbert, C. D.; Stelling, F. H. Potential of ceramic materials as permanently implantable skeletal prostheses. *J Biomed Mater Res* **1970**, *4*, 433–456. https://doi.org/10.1002/jbm.820040309
134. Bobyn, J. D.; Pilliar, R. M.; Cameron, H. U.; Weatherly, G. C. The optimum pore size for the fixation of porous-surfaced metal implants by the ingrowth of bone. *Clinical Orthopaedics and Related Research* **1980**, *150*.
135. Pilliar, R.M. Porous-surfaces metallic implants for orthopedic applications. *J. Biomed. Mater. Res.* **1987,** *21*(A1 Suppl), 1– 33.
136. Lu, J. X.; Flautre, B.; Anselme, K.; Gallur, A.; Descamps, M.; Thierry, B.; Hardouin, P. Study of porous interconnections of bioceramic on cellular rehabilitation in vitro and in vivo. *Bioceramics* **1997**, 583–586.
137. Itälä, A.I.; Ylänen, H.O.; Ekholm, C.; Karlsson, K.H.; Aro, H.T. Pore diameter of more than 100 μm is not requisite for bone ingrowth in Rabbits. *J. Biomed. Mater. Res.* **2001**, *58*, 679–683. https://doi.org/10.1002/jbm.106
138. Jones, A. C.; Arns, C. H.; Hutmacher, D. W.; Milthorpe, B. K.; Sheppard, A. P.; Knackstedt, M. A. The correlation of pore morphology, interconnectivity and physical properties of 3D ceramic scaffolds with bone ingrowth. *Biomaterials* **2009**, *30*, 1440–1451. https://doi.org/10.1016/j.biomaterials.2008.10.056
139. Chang, B.; Song, W.; Han, T.; Yan, J.; Li, F.; Zhao, L.; Kou, H.; Zhang, Y. Influence of pore size of porous titanium fabricated by vacuum diffusion bonding of titanium meshes on cell penetration and Bone Ingrowth. *Acta Biomater.* **2016**, *33*, 311–321. https://doi.org/10.1016/j.actbio.2016.01.022
140. Xue, W.; Krishna, B. V.; Bandyopadhyay, A.; Bose, S. Processing and biocompatibility evaluation of laser processed porous titanium. *Acta Biomaterialia* **2007**, *3*, 1007–1018. https://doi.org/10.1016/j.actbio.2007.05.009
141. Knychala, J.; Bouropoulos, N.; Catt, C. J.; Katsamenis, O. L.; Please, C. P.; Sengers, B. G. Pore geometry regulates early stage human bone marrow cell tissue formation and organisation. *Ann Biomed Eng* **2013**, *41*, 917–930. https://doi.org/10.1007/s10439-013-0748-z
142. Lu, X.; Wang, Y.; Jin, F. Influence of a non-biodegradable porous structure on Bone Repair. *RSC Advances* **2016**, *6*, 80522–80528. https://doi.org/10.1039/C6RA17747F
143. Shor, L.; Güçeri, S.; Wen, X.; Gandhi, M.; Sun, W. Fabrication of three-dimensional polycaprolactone/hydroxyapatite tissue scaffolds and osteoblast-scaffold interactions in vitro. *Biomaterials* **2007**, *28*, 5291–5297. https://doi.org/10.1016/j.biomaterials.2007.08.018
144. Dias, M. R.; Fernandes, P. R.; Guedes, J. M.; Hollister, S. J. Permeability analysis of scaffolds for bone tissue engineering. *Journal of Biomechanics* **2012**, *45*, 938–944. https://doi.org/10.1016/j.jbiomech.2012.01.019

145. Porter, A. E.; Buckland, T.; Hing, K.; Best, S. M.; Bonfield, W. The structure of the bond between bone and porous silicon-substituted hydroxyapatite bioceramic implants. *Journal of Biomedical Materials Research Part A* **2006**, *78A*, 25–33. https://doi.org/10.1002/jbm.a.30690
146. Karageorgiou, V.; Kaplan, D. Porosity of 3D biomaterial scaffolds and osteogenesis. *Biomaterials* **2005**, *26*, 5474–5491. https://doi.org/10.1016/j.biomaterials.2005.02.002
147. Fukuda, A.; Takemoto, M.; Saito, T.; Fujibayashi, S.; Neo, M.; Pattanayak, D. K.; Matsushita, T.; Sasaki, K.; Nishida, N.; Kokubo, T.; Nakamura, T. Osteoinduction of porous Ti implants with a channel structure fabricated by selective laser melting. *Acta Biomaterialia* **2011**, *7*, 2327–2336. https://doi.org/10.1016/j.actbio.2011.01.037
148. Wauthle, R.; van der Stok, J.; Amin Yavari, S.; Van Humbeeck, J.; Kruth, J.-P.; Zadpoor, A. A.; Weinans, H.; Mulier, M.; Schrooten, J. Additively manufactured porous tantalum implants. *Acta Biomater.* **2015**, *14*, 217–225. https://doi.org/10.1016/j.actbio.2014.12.003
149. Wally, Z. J.; Haque, A. M.; Feteira, A.; Claeyssens, F.; Goodall, R.; Reilly, G. C. Selective laser melting processed ti6al4v lattices with graded porosities for Dental Applications. *J. Mech. Behav. Biomed. Mater.* **2019**, *90*, 20–29. https://doi.org/10.1016/j.jmbbm.2018.08.047
150. Taniguchi, N.; Fujibayashi, S.; Takemoto, M.; Sasaki, K.; Otsuki, B.; Nakamura, T.; Matsushita, T.; Kokubo, T.; Matsuda, S. Effect of pore size on bone ingrowth into porous titanium implants fabricated by additive manufacturing: An in vivo experiment. *Mater. Sci. Eng. C* **2016**, *59*, 690–701. https://doi.org/10.1016/j.msec.2015.10.069
151. Wieding, J.; Lindner, T.; Bergschmidt, P.; Bader, R. Biomechanical stability of novel mechanically adapted open-porous titanium scaffolds in metatarsal bone defects of sheep. *Biomaterials* **2015**, *46*, 35–47. https://doi.org/10.1016/j.biomaterials.2014.12.010
152. Li, F.; Li, J.; Xu, G.; Liu, G.; Kou, H.; Zhou, L. Fabrication, pore structure and compressive behavior of anisotropic porous titanium for human trabecular bone implant applications. *J. Mech. Behav. Biomed. Mater.* **2015**, *46*, 104–114. https://doi.org/10.1016/j.jmbbm.2015.02.023
153. Chen, Z.; Yan, X.; Yin, S.; Liu, L.; Liu, X.; Zhao, G.; Ma, W.; Qi, W.; Ren, Z.; Liao, H.; Liu, M.; Cai, D.; Fang, H. Influence of the pore size and porosity of selective laser melted ti6al4v Eli porous scaffold on cell proliferation, osteogenesis and bone ingrowth. *Mater. Sci. Eng. C* **2020**, *106*, 110289. https://doi.org/10.1016/j.msec.2019.110289
154. Huang, G.; Pan, S.-T.; Qiu, J.-X. The osteogenic effects of porous tantalum and titanium alloy scaffolds with different unit cell structure. *Colloids and Surfaces B: Biointerfaces* **2022**, *210*, 112229. https://doi.org/10.1016/j.colsurfb.2021.112229
155. Lee, Y.; Jung, A.; Heo, S.-J.;Gweon, B.; Lim, D. Influences of surface topography of porous titanium scaffolds manufactured by powder bed fusion on osteogenesis. *J. Mater. Res. Technol.* **2023**, *23*, 2784–2797. https://doi.org/10.1016/j.jmrt.2023.01.153
156. Otsuki, B.; Takemoto, M.; Fujibayashi, S.; Neo, M.; Kokubo, T.; Nakamura, T. Pore throat size and connectivity determine bone and tissue ingrowth into porous implants: three-dimensional micro-CT based structural analyses of porous bioactive titanium implants. *Biomaterials*. **2006**, *27*, 5892–900. https://doi.org/10.1016/j.biomaterials.2006.08.013
157. Takemoto, M.; Fujibayashi, S.; Neo, M.; Suzuki, J.; Kokubo, T.; Nakamura, T. Mechanical properties and osteoconductivity of porous bioactive titanium. *Biomaterials*. **2005**, 30, 6014–6023. https://doi.org/10.1016/j.biomaterials.2005.03.019
158. Habibovic, P.; Li, J.; van der Valk, C.M.; Meijer, G.; Layrolle, P.; van Blitterswijk, C.A.; de Groot, K. Biological performance of uncoated and octacalcium phosphate-coated Ti6Al4V. *Biomaterials*. **2005**, *26*, 23–36. https://doi.org/10.1016/j.biomaterials.2004.02.02
159. Baino, F.; Yamaguchi, S. The Use of Simulated Body Fluid (SBF) for Assessing Materials Bioactivity in the Context of Tissue Engineering: Review and Challenges. *Biomimetics*. **2020**, *5*, 57. https://doi.org/10.3390/biomimetics5040057
160. Groeger, S.; Meyle, J. Reactivity of Titanium Dental Implant Surfaces in Simulated Body Fluid. *ACS Appl. Bio. Mater*. **2021**, *4*, 5575–5584. https://doi.org/10.1021/acsabm.1c00395
161. Kon, M.; Hirakata, L.M.; Asaoka, K. Porous Ti-6Al-4 V alloy fabricated by spark plasma sintering for biomimetic surface modification. *J. Biomed Mater. Res. B Appl. Biomater*. **2004**, *68*, 88–93. https://doi.org/10.1002/jbm.b.20004
162. Phillips, A.M. Overview of the fracture healing cascade. *Injury*. **2005**, 36, S5–7. https://doi.org/10.1016/j.injury.2005.07.027
163. Ai-Aql, Z.S.; Alagl, A.S.; Graves, D.T.; Gerstenfeld, L.C.; Einhorn, T.A. Molecular mechanisms controlling bone formation during fracture healing and distraction osteogenesis. *J. Dent. Res*. **2008**, 87, 107–118. https://doi.org/10.1177/154405910808700215
164. Schmid GJ, Kobayashi C, Sandell LJ, Ornitz DM. Fibroblast growth factor expression during skeletal fracture healing in mice. *Dev. Dyn*. **2009**, *238*, 766–774. https://doi.org/10.1177/154405910808700215

165. Yu, Y.Y.; Lieu, S.; Lu, C.; Miclau, T.; Marcucio, R.S.; Colnot, C. Immunolocalization of BMPs, BMP antagonists, receptors, and effectors during fracture repair. *Bone*. **2010**, *46*, 841–851. https://doi.org/10.1016/j.bone.2009.11.005
166. Burkus, J.K.; Gornet, M.F.; Dickman, C.A.; Zdeblick, T.A. Anterior lumbar interbody fusion using rhBMP-2 with tapered interbody cages. *J. Spinal Disord. Tech*. **2002**, *15*, 337–349. https://doi.org/10.1097/00024720-200210000-00001
167. Burkus, J.K.; Transfeldt, E.E.; Kitchel, S.H.; Watkins, R.G.; Balderston, R.A. Clinical and radiographic outcomes of anterior lumbar interbody fusion using recombinant human bone morphogenetic protein-2. *Spine*. **2002**, *27*, 2396–2408. https://doi.org/10.1097/00007632-200211010-00015
168. Turgeman, G.; Zilberman, Y.; Zhou, S.; Kelly, P.; Moutsatsos, I.K.; Kharode, Y.P.; Borella, L.E.; Bex, F.J.; Komm, B.S.; Bodine, P.V. et al. Systemically administered rhBMP-2 promotes MSC activity and reverses bone and cartilage loss in osteopenic mice. *J. Cell Biochem*. **2002**. *86*, 461–474. https://doi.org/10.1002/jcb.10231
169. Dumic-Cule, I.; Brkljacic, J.; Rogic, D.; Bordukalo, N.T.; Tikvica, L.A.; Draca, N.; Kufner, V.; Trkulja, V.; Grgurevic, L.; Vukicevic, S. Systemically available bone morphogenetic protein two and seven affect bone metabolism. *Int. Orthop*. **2014**, *38*, 1979–1985. https://doi.org/10.1007/s00264-014-2425-8
170. Akkiraju, H.; Bonor, J.; Olli, K.; Bowen, C.; Bragdon, B.; Coombs, H.; Donahue, L. R.; Duncan, R.; Nohe, A. Systemic injection of CK2.3, a novel peptide acting downstream of bone morphogenetic protein receptor bmpria, leads to increased trabecular bone mass. *J. Orthop. Res.* **2014**, 33, 208–215. https://doi.org/10.1002/jor.22752
171. Chen, D.; Zhao, M.; Mundy, G.R. Bone morphogenetic proteins. *Growth Factors*. **2004.** *22*, 233– 241, https://doi.org/10.1002/jor.22752
172. Lee, J.; Decker, J.F.; Polimeni, G.; Cortella, C.A.; Rohrer, M.D.; Wozney, J.M.; Hall, J.; Susin, C.; Wikesjo, U.M. Evaluation of implants coated with rhbmp-2 using two different coating strategies: a critical-size supraalveolar peri-implant defect study in dogs. *J. Clin. Periodontol.* **2010**, *37*, 582–590. https://doi.org/10.1111/j.1600-051X.2010.01557.x
173. Hunziker, E.B.; Jovanovic, J.; Horner, A.; Keel, M.J.; Lippuner, K.; Shintani, N. Optimisation of BMP-2 dosage for the osseointegration of porous titanium implants in an ovine model. *Eur. Cell Mater*. **2016**, *32*, 241–256. https://doi.org/10.22203/eCM.v032a16
174. Faundez, A.; Tournier, C.; Garcia, M.; Aunoble, S.; Le Huec, J.C. Bone morphogenetic protein use in spine surgery-complications and outcomes: a systematic review. *Int. Orthop*. **2016**, *40*, 1309–1319. https://doi.org/10.1007/s00264-016-3149-8
175. James, A.W.; LaChaud, G.; Shen, J.; Asatrian, G.; Nguyen, V.; Zhang, X.; Ting, K.; Soo, C. A review of the clinical side effects of bone morphogenetic protein-2. *Tissue Eng. Part. B. Rev*. **2016**, *22*, 284–297. https://doi.org/10.1089/ten.TEB.2015.0357
176. Hofstetter, C.P.; Hofer, A.S.; Levi, A.D. Exploratory meta-analysis on dose-related efficacy and morbidity of bone morphogenetic protein in spinal arthrodesis surgery. *J. Neurosurg Spine*. **2016**, *24*, 457–475. https://doi.org/10.3171/2015.4.SPINE141086
177. Vavken, J.; Mameghani, A.; Vavken, P.; Schaeren, S. Complications and cancer rates in spine fusion with recombinant human bone morphogenetic protein-2 (rhBMP-2). *Eur. Spine J*. **2015**, *25*, 3979–3989. https://doi.org/10.1007/s00586-015-3870- 9
178. Herberg, S.; Kondrikova, G.; Periyasamy-Thandavan, S.; Howie, R.N.; Elsalanty, M.E.; Weiss, L.; Campbell, P.; Hill, W.D.; Cray, J.J. Inkjet-based biopatterning of SDF-1β augments BMP-2-induced repair of critical size calvarial bone defects in mice. *Bone*. **2014**, *7*, 95–103. https://doi.org/10.1016/j.bone.2014.07.007
179. Pobloth, A.M.; Duda, G.N.; Giesecke, M.T.; Dienelt, A.; Schwabe, P. High-dose recombinant human bone morphogenetic protein-2 impacts histological and biomechanical properties of a cervical spine fusion segment: results from a sheep model. *J. Tissue Eng. Regen. Med*. **2017**, *11*, 1514–1523. https://doi.org/10.1002/term.204
180. Lin, H.S.; Pang, W.P.; Yuan, H.; Kong, Y.Z.; Long, F.L.; Zhang, R.Z.; Yang, L.; Fang, Q,L,; Pan, A.P.; Fan, X.H.; Li, M.F. Molecular subtypes based on DNA sensors predict prognosis and tumor immunophenotype in hepatocellular carcinoma. *Aging (Albany NY)*. **2023.** *14*, 15. https://doi.org/10.18632/aging.204870
181. Aro, H.T.; Govender, S.; Patel, A.D.; Hernigou, P.; Perera de Gregorio, A.; Popescu, G.I.; Golden, J.D.; Christensen, J.; Valentin, A. Recombinant human bone morphogenetic protein-2: a randomized trial in open tibial fractures treated with reamed nail fixation. *J. Bone Joint. Surg. Am*. **2011**, *93*, 801–808. https://doi.org/10.2106/JBJS.I.01763. E 3: 801–808
182. Mroz, T.E.; Wang, J.C.; Hashimoto, R.; Norvell, D.C. Complications related to osteobiologics use in spine surgery: a systematic review. *Spine*. **2010**, *35*, S86–S104. https://doi.org/10.1097/BRS.0b013e3181edf576
183. Guillot, R.; Gilde, F.; Becquart, P.; Sailhan, F.; Lapeyrere, A.; Logeart-Avramoglou, D.; Picart, C. The stability of BMP loaded polyelectrolyte multilayer coatings on titanium. *Biomaterials*. **2013**, *34*, 5737–5746. https://doi.org/10.1016/j.biomaterials.2013.03.06

184. Baltzer, A.W.; Lattermann, C.; Whalen, J.D.; Ghivizzani, S.; Wooley, P.; Krauspe, R.; Robbins, P.D.; Evans, C.H. Potential role of direct adenoviral gene transfer in enhancing fracture repair. *Clin. Orthop. Relat. Res.* **2000**, *379*, S120–S125. https://doi.org/10.1097/00003086-200010001-00016
185. Zhao, M.; Zhao, Z.; Koh, J.T.; Jin, T.; Franceschi, R.T. Combinatorial gene therapy for bone regeneration: cooperative interactions between adenovirus vectors expressing bone morphogenetic proteins 2, 4, and 7. *J. Cell Biochem*. **2005**, *95*, 1–16. https://doi.org/10.1002/jcb.20411
186. Lutz, R.; Park, J.; Felszeghy, E.; Wiltfang, J.; Nkenke, E.; Schlegel, K.A. Bone regeneration after topical bmp-2-gene delivery in circumferential peri-implant bone defects. *J. Clin. Oral Implants Res.* **2008**, *19*, 590–559. https://doi.org/10.1111/j.1600-0501.2007.01526.x
187. Chen, C.F.; Chen ,Y.C.; Fu, Y.S.; Tsai, S.W.; Wu, P.K.; Chen, C.M.; Chang, M.C.; Chen, W.M. Characterization of Osteogenesis and Chondrogenesis of Human Decellularized Allogeneic Bone with Mesenchymal Stem Cells Derived from Bone Marrow, Adipose Tissue, and Wharton's Jelly. *Int. J. Mol. Sci*. **2021**, *22*, 8987. https://doi.org/10.3390/ijms22168987
188. Cohen, D.J.; Cheng, A.; Sahingur, K.; Clohessy, R.M.; Hopkins, L.B.; Boyan, B.D.; Schwartz, Z. Performance of laser sintered Ti-6Al-4V implants with bone-inspired porosity and micro/nanoscale surface roughness in the rabbit femur. *Biomed. Mater*. **2017**, *12*, 025021. https://doi.org/10.1088/1748-605X/aa6810
189. Sakisaka, Y.; Ishihata, H.; Maruyama, K.; Nemoto, E.; Chiba, S.; Nagamine, M.; Hasegawa, H.; Hatsuzawa, T.; Yamada, S. Serial Cultivation of an MSC-Like Cell Line with Enzyme-Free Passaging Using a Microporous Titanium Scaffold. *Materials* **2023**, *16*, 1165. https://doi.org/10.3390/ma16031165
190. Yuan, B.; Liu, P.; Zhao, R.; Yang, X.; Xiao, Z.; Zhang, K; Zhu, X.; Zhang, X. Functionalized 3D-printed porous titanium scaffold induces in situ vascularized bone regeneration by orchestrating bone microenvironment. *J. Mater. Sci. Techol*. **2023**, *153*, 92–105. https://doi.org/10.1016/j.jmst.2022.12.033
191. Steiner, D.; Reinhardt, L.; Fischer, L.; Popp, V.; Körner, C.; Geppert, C.I.; Bäuerle, T.; Horch, R.E.; Arkudas, A. Impact of Endothelial Progenitor Cells in the Vascularization of Osteogenic Scaffolds. *Cells* **2022**, *11*, 926. https://doi.org/10.3390/cells1106092
192. Seebach, C.; Henrich, D.; Kahling, C.; Wilhelm, K.; Tami, A.E.; Alini, M.; Marzi, I. Endothelial progenitor cells and mesenchymal stem cells seeded onto β-TCP granules enhance early vascularization and bone healing in a critical-sized bone defect in rats. *Tissue Eng. Part. A*. **2010**, *16*, 1961–1970. https://doi.org/10.1089/ten.tea.2009.0715
193. Duffy, G.P.; Ahsan, T.; O'Brien, T.; Barry, F.; Nerem, R.M. Bone marrow-derived mesenchymal stem cells promote angiogenic processes in a time- and dose-dependent manner in vitro. *Tissue Eng. Part. A.* **2009**, *15*, 2459–2470. https://doi.org/10.1089/ten.tea.2008.0341
194. Arts, M.; Torensma, B.; Wolfs, J. Porous titanium cervical interbody fusion device in the treatment of degenerative cervical radiculopathy; 1-year results of a prospective controlled trial. *Spine J*. **2020,** *20*, 1065–1072. https://doi.org/10.1016/j.spinee.2020.03.008
195. Wang, Y.; Zhou, Y.; Chai, X.; Zhuo, H. Application of three-dimensional printed porous titanium alloy cage and poly-ether-ether-ketone cage in posterior lumbar interbody fusion. **2022**, *36*, 1126–1131. https://doi.org/10.7507/1002-1892.202204011
196. Arts, M.; Torensma, B.; Wolfs, J. Porous titanium cervical interbody fusion device in the treatment of degenerative cervical radiculopathy; 1-year results of a prospective controlled trial. *Spine J*. **2020** *20*, 1065–1072. https://doi.org/10.1016/j.spinee.2020.03.008
197. Salemyr, M.; Muren, O.; Eisler, T.; Bodén, H.; Chammout, G.; Stark, A.; Sköldenberg, O. Porous titanium construct cup compared to porous coated titanium cup in total hip arthroplasty. A randomised controlled trial. *Int. Orthop*. **2015**, *39*, 823–832. https://doi.org/10.1007/s00264-014-2571-z
198. Yoshioka, S.; Nakano, S.; Kinoshita, Y.; Nakamura, M.; Goto, T.; Hamada, D.; Sairyo, K. Comparison of a highly porous titanium cup (Tritanium) and a conventional hydroxyapatite-coated porous titanium cup: A retrospective analysis of clinical and radiological outcomes in hip arthroplasty among Japanese patients. *J. Orthop. Sci*. **2018**, *23*, 967–972. https://doi.org/10.1016/j.jos.2018.06.018.